

A General Control-Theoretic Approach for Reinforcement Learning: Theory and Algorithms

Wei Qin Chen

CHENW18@RPI.EDU

Department of Electrical, Computer, and Systems Engineering, Rensselaer Polytechnic Institute

Mark S. Squillante

MSS@US.IBM.COM

Mathematical Sciences Department, IBM Research

Chai Wah Wu

CWWU@US.IBM.COM

Mathematical Sciences Department, IBM Research

Santiago Paternain

PATERS@RPI.EDU

Department of Electrical, Computer, and Systems Engineering, Rensselaer Polytechnic Institute

Abstract

We devise a control-theoretic reinforcement learning approach to support direct learning of the optimal policy. We establish various theoretical properties of our approach, such as convergence and optimality of our analog of the Bellman operator and Q -learning, a new control-policy-variable gradient theorem, and a specific gradient ascent algorithm based on this theorem within the context of a specific control-theoretic framework. We empirically evaluate the performance of our control-theoretic approach on several classical reinforcement learning tasks, demonstrating significant improvements in solution quality, sample complexity, and running time of our approach over state-of-the-art methods.

Keywords: Reinforcement learning, Control theory, Q -learning, Policy gradient methods

1. Introduction

For many years now, numerous reinforcement learning (RL) approaches, with differing degrees of success, have been developed to address a wide variety of decision making under uncertainty problems (Feng et al., 2024; Kaelbling et al., 1996; McMahan et al., 2024; Shen, 2024; Szepesvari, 2010; Sutton and Barto, 2020; Zheng et al., 2023). Model-free RL methods (Randlov and Alstrom, 1998; Mnih et al., 2013) can often suffer from high sample complexity that may require an inordinate amount of samples for some problems, making them unsuitable for various applications where collecting large amounts of data is time-consuming, costly and potentially dangerous for the system and its surroundings (Zhang and Tan, 2024; Chen et al., 2024; Peng et al., 2023; Dong et al., 2023; Kumar et al., 2020). On the other hand, model-based RL methods have been successful in demonstrating significantly reduced sample complexity and in outperforming model-free approaches for various decision making under uncertainty problems; see, e.g., Deisenroth and Rasmussen (2011); Meger et al. (2015). However, such model-based approaches can suffer from the difficulty of learning an appropriate model and from worse asymptotic performance than model-free approaches due to model bias from inherently assuming the learned system dynamics model accurately represents the true system environment; see, e.g., Atkeson and Santamaria (1997); Schneider (1997); Schaal (1997).

In this paper, we propose a novel form of RL that exploits optimal control-theoretic methods to solve the general problem formulation in terms of the unknown independent variables of the

underlying control problem and that directly learns these unknown variables through an iterative solution process that applies the corresponding optimal control policy. This general approach is in strong contrast to many traditional model-based RL methods that, after learning the system dynamics model which is often of high complexity and dimensionality, then use this system dynamics model to compute an approximate solution of a corresponding (stochastic) dynamic programming problem, often applying model predictive control; see, e.g., [Nagabandi et al. \(2018\)](#). Our control-based RL (CBRL) approach instead directly learns the unknown independent variables of the general underlying (unknown) dynamical system from which we derive the optimal control policy, often of much lower complexity and dimensionality, through control-theoretic means.

The theoretical foundation and analysis of our CBRL approach are presented within the context of a general Markov decision process (MDP) framework that *(i)* extends the methodology from the family of policies associated with the classical Bellman operator to a family of control-policy functions mapping a vector of (unknown) variables from a corresponding independent variable set to a control policy which is optimal under those variables; and *(ii)* extends the domain of these control policies from a single state to span across all (or a large subset of) states, with the (unknown) variable vector encoding global and local information that needs to be learned. Within the context of this MDP framework and our general CBRL approach, we establish theoretical results on convergence and optimality with respect to (w.r.t.) a CBRL operator and a CBRL version of Q -learning, analogous to corresponding results for the Bellman operator and classical Q -learning, respectively.

One might potentially consider our CBRL approach to be somewhat related to previous efforts on learning a parameterized policy within an MDP framework to reduce sample complexity, such as policy gradient methods ([Sutton et al., 1999](#); [Sutton and Barto, 2020](#)) and their variants including neural network based policy optimization approaches ([Schulman et al., 2015, 2017](#); [Agarwal et al., 2021](#)). Despite any potentially perceived similarities, it is important to note that our CBRL approach is fundamentally different from policy gradient methods in several important ways. More specifically, *(i)* we do not consider parameterized policies within the general MDP framework, *(ii)* we instead exploit control-theoretic methods to derive the optimal policy in terms of estimates of a few unknown (global and local) independent variables of the corresponding control problem, and *(iii)* we directly learn these unknown variables in an iterative manner based on observations from applying the optimal control policy for the current estimate of variables. Meanwhile, within the context of our general CBRL approach, we establish a new control-policy-variable gradient theorem, analogous to the standard policy gradient theorem, together with a corresponding gradient ascent method that comprises an iterative process for directly learning the (unknown) variable vector.

With its foundation being optimal control, our CBRL approach is particularly suitable for dynamical systems in general and thereby provides the optimal control policy for a wide variety of systems. In addition to its established theoretical properties, numerical experiments of various classical decision making under uncertainty tasks empirically demonstrate the effectiveness and performance benefits of our CBRL approach in reducing the number of samples needed, which is a key requirement for the application of learning and decision-making algorithms in real-world systems.

The remainder of the paper is organized as follows. We first present our general CBRL approach, which includes establishing various theoretical properties of our approach. Numerical results are presented next, followed by concluding remarks. All proofs and additional details and results are provided in the appendices.

2. CBRL Approach

Consider a standard RL framework (see, e.g., Sutton and Barto (2020); Bertsekas and Tsitsiklis (1996)) in which a decision-making agent interacts with a stochastic environment modeled as an MDP defined over a set of states \mathbb{X} , a set of actions \mathbb{U} , a transition probability kernel \mathbb{P} , and a reward function r mapping state-action pairs to a bounded subset of \mathbb{R} . The agent seeks to determine a policy $\pi(\cdot|x) : \mathbb{X} \rightarrow \mathbb{U}$ comprising the sequence of control actions u_1, u_2, \dots that maximizes a discounted infinite-horizon stochastic dynamic programming (sDP) formulation expressed as

$$\max_{u_1, u_2, \dots} \mathbb{E}_{\mathbb{P}} \left[\sum_{t=0}^{\infty} \gamma^t r(x_t, u_t) \right], \quad (1)$$

where $x_t \in \mathbb{X}$ denotes the state of the system at time $t \in \mathbb{Z}_+$, $u_t \in \mathbb{U}$ the control action at time t , $\gamma \in (0, 1)$ the discount factor, and $\mathbb{E}_{\mathbb{P}} := \mathbb{E}_{x_{t+1} \sim \mathbb{P}(\cdot|x_t, u_t)}$ defines expectation w.r.t. the conditional transition probability for the next state $\mathbb{P}(\cdot|x_t, u_t)$. The deterministic policy $\pi(\cdot|x) : \mathbb{X} \rightarrow \mathbb{U}$ defines the control action given the current state x , for which we simply write $\pi(x)$. Let $\mathbb{Q}(\mathbb{X} \times \mathbb{U})$ denote the space of bounded real-valued functions over $\mathbb{X} \times \mathbb{U}$ with supremum norm, and let Π denote the set of all stationary policies. From standard theory, define the Bellman operator \mathcal{T}_B on $\mathbb{Q}(\mathbb{X} \times \mathbb{U})$ as

$$\mathcal{T}_B Q(x, u) := r(x, u) + \gamma \mathbb{E}_{\mathbb{P}} \max_{u' \in \mathbb{U}} Q(x', u'), \quad (2)$$

where x' denotes the next state upon transition from x ; we note that (2) is also referred to in the research literature as the Bellman optimality operator. Define $Q^*(x, u)$, $V^*(x) := \max_{u \in \mathbb{U}} Q^*(x, u)$, and $\pi^*(x) := \arg \max_{u \in \mathbb{U}} Q^*(x, u)$ to be the optimal action-value function, the optimal value function, and the optimal deterministic stationary policy, respectively.

Our CBRL approach consists of exploiting control-theoretic methods to solve the general sDP formulation (1) in terms of the corresponding unknown independent variables, and directly learning these unknown variables over time through an associated iterative solution process. In particular, our general approach considers two key ideas: (i) extending the solution methodology from the family of policies Π associated with classical RL to a family of control-policy functions that map a variable vector v from an independent variable set to a control policy that is optimal under the independent variable vector v ; and (ii) extending the domain of these control policies from a single state to span across all (or a large subset of) states in \mathbb{X} , with the independent variable vector v encoding both global and local information (e.g., gravity and mass) that is unknown and needs to be learned.

More formally, let \mathbb{V} denote a subset of a metric space serving as the set of variable vectors, and \mathbb{F} the family of control-policy functions whose elements comprise surjective functions $\mathcal{G} : v \mapsto \mathcal{F}_v$ that map a variable vector $v \in \mathbb{V}$ to a control policy $\mathcal{F}_v : \mathbb{X} \rightarrow \mathbb{U}$ that is optimal under v . Let $\tilde{\Pi} \subseteq \Pi$ denote the set of all stationary policies that are directly determined by the control-policy functions $\mathcal{G}(v)$ over all $v \in \mathbb{V}$. For any $v \in \mathbb{V}$, the control-policy function $\mathcal{G}(\cdot) \in \mathbb{F}$ derives a particular control policy $\mathcal{F}_v \in \tilde{\Pi}$ that provides the best expected cumulative discounted reward across all states $x \in \mathbb{X}$ from among all control-policy functions in \mathbb{F} . Such control policy mappings $\mathcal{G} : \mathbb{V} \rightarrow \tilde{\Pi}$ derive optimal control policies from vectors in the variable set \mathbb{V} through control-theoretic methods, with the goal of learning the unknown variable vector $v \in \mathbb{V}$ through a corresponding iterative solution process. Hence, once the variable vector is learned with sufficient accuracy, the desired optimal control policy is realized.

The control policy mappings $\mathcal{G}(\cdot)$ that derive an optimal control policy for each independent-variable vector $v \in \mathbb{V}$ come from a specific control-theoretic framework chosen to be combined as

part of our CBRL approach for this purpose. In practice, this selected control-theoretic framework of interest may be an approximation and not provably optimal for the underlying sDP formulation (1), as long as it is sufficiently accurate for the RL task at hand. As a representative example, we focus in this paper on our CBRL approach in combination with the linear quadratic regulator (LQR) framework within which the system dynamics are linear and the objective function is quadratic. More formally, the LQR system dynamics are governed by $\dot{x} = A_v x + B_v u$ with initial state x_0 , where the vector v is contained in the matrices A_v and B_v ; and the LQR objective function to be minimized is given by $\int_0^\infty (x_t^\top \underline{Q}_v x_t + u_t^\top R_v u_t) dt$, where the vector v may be contained in the matrices \underline{Q}_v and R_v . Here the matrices A_v and B_v respectively define the linear system dynamics and the linear system control; and the matrices $\underline{Q}_v = \underline{Q}_v^\top \succeq 0$ and $R_v = R_v^\top \succ 0$ respectively define the quadratic system costs and the quadratic control costs. Within the context of this LQR framework, the vector v comprises the d unknown real-valued independent variables contained in the LQR problem formulations, and thus the independent variable set $\mathbb{V} \subseteq \mathbb{R}^d$; the family of control-policy functions \mathbb{F} comprises all mappings from \mathbb{V} to the corresponding set of LQR problem formulations (i.e., $\mathbb{F} = \{(\min P_v), \forall v \in \mathbb{V}\}$, where $P_v := \int_0^\infty (x^\top \underline{Q}_v x + u^\top R_v u) dt$, $\dot{x} = A_v x + B_v u$); and the control-policy function $\mathcal{G}(\cdot) \in \mathbb{F}$ maps a given v to the specific corresponding LQR problem formulation (i.e., $\mathcal{G}(v) = (\min P_v)$, for fixed $v \in \mathbb{V}$), whose solution is the linear control policy $\mathcal{F}_v \in \tilde{\Pi}$ (i.e., $\mathcal{F}_v = (\arg \min P_v)$, for fixed $v \in \mathbb{V}$) which renders the action $\mathcal{F}_v(x)$ taken in state $x \in \mathbb{X}$.

In the remainder of this section, we establish various theoretical properties of our CBRL approach including convergence, optimality, and control-policy-variable gradient ascent.

2.1. Convergence and Optimality

We consider an analog of the Bellman operator \mathcal{T}_B within our general CBRL approach and derive a set of related theoretical results on convergence and optimality. For each Q -function $q(x, u) \in \mathbb{Q}(\mathbb{X} \times \mathbb{U})$, we define the generic CBRL function $\tilde{q} : \mathbb{X} \times \tilde{\Pi} \rightarrow \mathbb{R}$ as $\tilde{q}(x, \mathcal{F}_v) := q(x, \mathcal{F}_v(x))$ where the control policy \mathcal{F}_v is derived from the control-policy function \mathcal{G} for a given variable vector $v \in \mathbb{V}$, and thus $\tilde{q}(x, \mathcal{F}_v) \in \tilde{\mathbb{Q}}(\mathbb{X} \times \tilde{\Pi})$ with $\tilde{\mathbb{Q}}(\mathbb{X} \times \tilde{\Pi})$ denoting the space of bounded real-valued functions over $\mathbb{X} \times \tilde{\Pi}$ with supremum norm. We then define our CBRL operator \mathbf{T} on $\tilde{\mathbb{Q}}(\mathbb{X} \times \tilde{\Pi})$ as

$$(\mathbf{T}\tilde{q})(x, \mathcal{F}_v) := \sum_{y \in \mathbb{X}} \mathbb{P}(y | x, \mathcal{F}_v) \left[r(x, \mathcal{F}_v(x)) + \gamma \sup_{v' \in \mathbb{V}} \tilde{q}(y, \mathcal{F}_{v'}) \right]. \quad (3)$$

Our approach comprises a sequence of steps from the family \mathbb{F} to the control-policy functions $\mathcal{G} \in \mathbb{F}$ to the control policies $\mathcal{F}_v \in \tilde{\Pi}$ to the control action $\mathcal{F}_v(x) \in \mathbb{U}$, upon applying \mathcal{F}_v in state $x \in \mathbb{X}$. It is important to note that the supremum in (3) is taken over all independent-variable vectors in \mathbb{V} , where the control-policy function $\mathcal{G}(v')$ for each $v' \in \mathbb{V}$ derives through control-theoretic means the corresponding control policy $\mathcal{F}_{v'}$, and thus taking the supremum over \mathbb{V} in (3) is equivalent to taking the supremum over $\tilde{\Pi}$. We next introduce an important assumption on the richness of the family \mathbb{F} within the sequence of steps of our approach from \mathbb{F} to $\mathcal{F}_v(x)$.

Assumption 1 *There exist a policy function \mathcal{G} in the family \mathbb{F} and a unique variable vector v^* in the independent-variable set \mathbb{V} such that, for any state $x \in \mathbb{X}$, $\pi^*(x) = \mathcal{F}_{v^*}(x) = \mathcal{G}(v^*)(x)$.*

Intuitively, Assumption 1 says that \mathbb{F} is rich enough to include a global control policy that coincides with the Bellman operator for each state. We then have the following formal result on the

convergence of the operator \mathbf{T} of our CBRL approach and the optimality of this convergence w.r.t. the Bellman equation (Sutton and Barto, 2020; Bertsekas and Tsitsiklis, 1996).

Theorem 1 *For any $\gamma \in (0, 1)$, the operator \mathbf{T} in (3) is a contraction in the supremum norm. Supposing Assumption 1 holds for the family of policy functions \mathbb{F} and its variable set \mathbb{V} , the contraction operator \mathbf{T} achieves the same asymptotically optimal outcome as that of the Bellman operator \mathcal{T}_B .*

Theorem 1 implies that, under the contraction operator \mathbf{T} and Assumption 1, our CBRL approach is optimal by realizing the same unique fixed point of the Bellman operator \mathcal{T}_B . In particular, from Theorem 1 for any function $\tilde{q} \in \tilde{\mathcal{Q}}(\mathbb{X} \times \tilde{\Pi})$, the iterations $\mathbf{T}^t(\tilde{q})$ converge as $t \rightarrow \infty$ to $\tilde{q}^*(x, \mathcal{F}_v)$, the unique optimal fixed point of the CBRL operator \mathbf{T} , and $\tilde{q}^*(x, \mathcal{F}_v)$ satisfies

$$\tilde{q}^*(x, \mathcal{F}_v) = \sum_{y \in \mathbb{X}} \mathbb{P}(y | x, \mathcal{F}_v) \left[r(x, \mathcal{F}_v(x)) + \gamma \sup_{v' \in \mathbb{V}} \tilde{q}^*(y, \mathcal{F}_{v'}) \right]. \quad (4)$$

We note, however, that this optimality is achieved with great reduction in the sample complexity due in part to another important difference with standard RL, namely the search of our CBRL approach across all states $x \in \mathbb{X}$ to find an optimal independent-variable vector v^* that identifies a single optimal control-policy function $\mathcal{G}^* \in \mathbb{F}$ which coincides with the Bellman equation for each state.

Now consider convergence of the Q -learning algorithm within the context of our general CBRL approach, where we focus on the following CBRL version of the classical Q -learning update rule (Watkins, 1989):

$$\tilde{q}_{t+1}(x_t, \mathcal{F}_{v,t}) = \tilde{q}_t(x_t, \mathcal{F}_{v,t}) + \alpha_t(x_t, \mathcal{F}_{v,t}) \left[r_t + \gamma \sup_{v' \in \mathbb{V}} \tilde{q}_t(x_{t+1}, \mathcal{F}_{v'}) - \tilde{q}_t(x_t, \mathcal{F}_{v,t}) \right], \quad (5)$$

for $0 < \gamma < 1$, $0 \leq \alpha_t(x_t, \mathcal{F}_{v,t}) \leq 1$ and iterations t . Let $\{\mathcal{F}_{v,t}\}$ be a sequence of control policies that covers all state-action pairs and r_t the corresponding reward of applying $\mathcal{F}_{v,t}$ to state x_t . We then have the following formal result on Q -learning convergence and the optimality of this convergence.

Theorem 2 *Suppose Assumption 1 holds for the family of policy functions \mathbb{F} and its independent-variable set \mathbb{V} with a contraction operator \mathbf{T} as defined in (3). If $\sum_t \alpha_t = \infty$, $\sum_t \alpha_t^2 < \infty$, and r_t are bounded, then \tilde{q}_t under the Q -learning update rule (5) converges to the optimal fixed point \tilde{q}^* as $t \rightarrow \infty$ and the optimal policy function is obtained from a unique variable vector $v^* \in \mathbb{V}$.*

Iterations t w.r.t. either the operator \mathbf{T} in (3) or the Q -learning update rule in (5) then consist of improving the estimates of the independent-variable vector v while applying the optimal control policy derived from the optimal control-policy function \mathcal{G} for the current variable vector estimate v_t based on the control-theoretic framework of interest. Within the context of the LQR control-theoretic framework as a representative example, it is well known from classical control theory that the solution of the corresponding sDP is determined by solving the algebraic Riccati equation (ARE) (Lancaster and Rodman, 1995), whose continuous-time version (CARE) is expressed as

$$A_v^\top P + P A_v - P B_v R_v^{-1} B_v^\top P + \underline{Q}_v = 0. \quad (6)$$

The optimal control policy action at iteration t , in system state x_t with independent-variable vector estimate v_t , is then obtained from the solution P of the CARE (6) as $\mathcal{F}_{v_t}(x_t) = -(R_{v_t}^{-1} B_{v_t}^\top P) x_t$, together with the change of coordinates $\tilde{x} = x - x^*$ in general when the target x^* is not the origin.

Before addressing in Section 2.2 one such iterative process to efficiently estimate the variable vector v , it is important to note that the control-theoretic framework selected to be combined as part of our CBRL approach need not be provably optimal for the RL task at hand. In particular, as long as the selected control-theoretic framework is sufficiently accurate, our approach can yield an approximate solution within a desired level of accuracy. To further support framework selection for such approximations, we first relax some of the above conditions to consider families \mathbb{F} that do not satisfy Assumption 1 and consider control-policy functions that map a variable vector to a control policy whose domain spans across a large subset of states (as opposed to all states) in \mathbb{X} and renders asymptotically optimal (as opposed to globally optimal) rewards. Supposing \mathbb{F} satisfies Assumption 1, consider a sequence of less rich families $\mathbb{F}_1, \mathbb{F}_2, \dots, \mathbb{F}_{k-1}, \mathbb{F}_k$ of policy functions $\mathcal{G}^{(i)} \in \mathbb{F}_i$ obtained from independent-variable vectors of the corresponding independent variable sets \mathbb{V}_i , and define the operators $\mathbf{T}_i : \tilde{\mathbb{Q}}(\mathbb{X} \times \tilde{\Pi}_i) \rightarrow \tilde{\mathbb{Q}}(\mathbb{X} \times \tilde{\Pi}_i)$ as in (3) for any function $\tilde{q}_i(x, \mathcal{F}_v^{(i)}) \in \tilde{\mathbb{Q}}(\mathbb{X} \times \tilde{\Pi}_i)$, $i \in [k] := \{1, \dots, k\}$. Then, from Theorem 1, each operator \mathbf{T}_i under variable set \mathbb{V}_i is a contraction in the supremum norm and converges to the unique fixed point $\tilde{q}_i^*(x, \mathcal{F}_v^{(i)})$ that satisfies the corresponding version of (4), for all $x \in \mathbb{X}$ and $v \in \mathbb{V}_i$, $i \in [k]$. We then have the following formal result on the asymptotic optimality of our CBRL approach in such approximate settings.

Theorem 3 *Assume the state and action spaces are compact and \mathcal{F}_v is uniformly continuous for each v . Consider \mathbb{F} and a sequence of families of policy functions $\mathbb{F}_1, \mathbb{F}_2, \dots, \mathbb{F}_{k-1}, \mathbb{F}_k$, with \mathbb{V} and \mathbb{V}_i respectively denoting the independent-variable sets corresponding to \mathbb{F} and \mathbb{F}_i , $i \in [k]$. Let $d(\cdot, \cdot)$ be a sup-norm distance function defined over the policy space $\tilde{\Pi}$, i.e., $d(\mathcal{F}_{v_i}^{(i)}, \mathcal{F}_{v_j}^{(j)}) = \sup_{x \in \mathbb{X}} \|\mathcal{F}_{v_i}^{(i)}(x) - \mathcal{F}_{v_j}^{(j)}(x)\|$, $v_i \in \mathbb{V}_i, v_j \in \mathbb{V}_j$. Further let $d'(\cdot, \cdot)$ be an inf-norm distance function defined over the policy function space \mathbb{F} , i.e., $d'(\mathcal{G}^{(i)}, \mathcal{G}^{(j)}) = \inf_{v_i \in \mathbb{V}_i, v_j \in \mathbb{V}_j} d(\mathcal{G}^{(i)}(v_i), \mathcal{G}^{(j)}(v_j))$, $\mathcal{G}^{(i)} \in \mathbb{F}_i, \mathcal{G}^{(j)} \in \mathbb{F}_j$. Suppose, for all $\mathcal{G} \in \mathbb{F}$, there exists a $\mathcal{G}^{(k)} \in \mathbb{F}_k$ such that $d'(\mathcal{G}^{(k)}, \mathcal{G}) \rightarrow 0$ as $k \rightarrow \infty$. Then, $\|\tilde{q}_k^* - \tilde{q}^*\|_\infty \rightarrow 0$ as $k \rightarrow \infty$.*

An analogous version of Theorem 3 based on Q -learning can be established in a similar manner w.r.t. Theorem 2, where the construction of the corresponding update rules in (5) under the variable sets \mathbb{V}_i parallels the above construction of the operators \mathbf{T}_i under the same variable sets \mathbb{V}_i . In the cases of both Theorem 3 and its Q -learning variant, one specific instance of a sequence of the families of policy functions $\mathbb{F}_1, \dots, \mathbb{F}_k$ consists of piecewise-linear control policies of increasing richness (e.g., the class of canonical piecewise-linear functions considered in (Lin and Unbehauen, 1992)) w.r.t. finer and finer granularity of the control policy function space converging towards \mathbb{F} .

2.2. Control-Policy-Variable Gradient Ascent

Turning now to our CBRL iterative process within the context of policy gradient methods, we build on our foregoing results to establish theoretical results analogous to the standard policy gradient theorem that establishes, for policies parameterized by θ , a connection between the gradient of the value function w.r.t. θ and the gradient of the policy action w.r.t. θ . This standard theoretical result does not apply to our CBRL approach because there is no direct connection between the independent-variable vector $v \in \mathbb{V}$ and the control policy action, as described above. Rather, under our CBRL approach and for any vector v , the control-policy function $\mathcal{G}(v) \in \mathbb{F}$ derives a particular control policy $\mathcal{F}_v \in \tilde{\Pi}$, and then the policy applied in any state $x \in \mathbb{X}$ yields the action taken.

So far, we have considered a deterministic control policy for the action taken at each state, since it is well known that a deterministic stationary policy is optimal for our sDP (1); refer to Puterman

(2005). For consistency with standard policy gradient methods, however, we consider in this subsection a general stochastic control policy that follows a probability distribution for the action taken at each state, where a deterministic policy is a special case. To this end, let us denote by \mathbb{W} a probability distribution on the set of actions \mathbb{U} where the stationary control policy $\mathcal{F}_v : \mathbb{X} \rightarrow \mathbb{W}$ defines a probability distribution over all available control actions $u \in \mathbb{U}$ given the current state $x \in \mathbb{X}$. Further define $\mathcal{F}_{v,u}(x)$ to be the element of $\mathcal{F}_v(x)$ corresponding to action u , i.e., $\mathcal{F}_{v,u}(x) := \mathbb{P}[u_t = u | x_t = x, \mathcal{F}_v]$, and correspondingly define $\tilde{q}_u(x, \mathcal{F}_v) := q_u(x, \mathcal{F}_v(x)) := q^v(x, u)$, where the latter denotes the Q -function of the policy \mathcal{F}_v . Let x_0 denote the start state at time $t = 0$ and $\mathbb{P}(x, k | x_0, \mathcal{F}_v)$ the probability of going from state x_0 to state x in k steps under the control policy \mathcal{F}_v . Our general control-policy-variable gradient ascent result is then formally expressed as follows.

Theorem 4 *Consider a family of control policy functions \mathbb{F} , its independent-variable set \mathbb{V} with contraction operator \mathbf{T} in the form of (3), and the value function $V_{\mathcal{F}_v}$ under the control policy \mathcal{F}_v . Assuming $\mathcal{F}_{v,u}(x)$ is differentiable w.r.t. \mathcal{F}_v and $\mathcal{F}_v(x)$ is differentiable w.r.t. v , we then have*

$$\nabla_v V_{\mathcal{F}_v}(x_0) = \sum_{x \in \mathbb{X}} \sum_{k=0}^{\infty} \gamma^k \mathbb{P}(x, k | x_0, \mathcal{F}_v) \left[\sum_{u \in \mathbb{U}} \frac{\partial \mathcal{F}_{v,u}(x)}{\partial \mathcal{F}_v} \frac{\partial \mathcal{F}_v(x)}{\partial v} \tilde{q}_u(x, \mathcal{F}_v) \right]. \quad (7)$$

The corresponding gradient ascent result for the case of deterministic control policies follows directly from Theorem 4 with the conditional probability distribution $\mathcal{F}_{v,u}(x)$ given by the associated indicator function $\mathbb{I}_{\mathcal{F}_v(x)}(u)$, returning 1 if and only if $u = \mathcal{F}_v(x)$ and zero otherwise.

Following along similar lines of the various forms of policy-gradient ascent methods based on the standard policy gradient theorem, we devise control-policy-variable gradient ascent methods within the context of our CBRL approach based on Theorem 4. One such gradient ascent method comprises an iterative process for directly learning the unknown independent-variable vector v of the optimal control policy w.r.t. the value function $V_{\mathcal{F}_v}$ whose iterations proceed according to

$$v_{t+1} = v_t + \eta \nabla_v V_{\mathcal{F}_v}(x_t), \quad (8)$$

where η is the step size and $\nabla_v V_{\mathcal{F}_v}$ is given by (7). Note that standard policy gradient methods are special cases of (8) where v_t is directly replaced by the policy π_t ; identity map for \mathcal{G} and $\frac{\partial V}{\partial \mathcal{F}_{v_t}} \frac{\partial \mathcal{F}_{v_t}}{\partial v_t}$ replaced by $\frac{\partial V}{\partial \pi_t}$ corresponds to the direct policy gradient parameterization in Agarwal et al. (2021).

More precisely, consider the iterative process of our control-policy-variable gradient ascent method above within the context of the LQR control-theoretic framework where at iteration t the system is in state x_t and the variable vector estimate is v_t . The optimal control policy \mathcal{F}_{v_t} is derived by solving for P in the corresponding CARE (6) and then setting $u_t^* = \mathcal{F}_{v_t}(x_t) = -Kx_t$, where $K = R_{v_t}^{-1} B_{v_t}^\top P$, together with the change of coordinates $\tilde{x} = x - x^*$ whenever the target x^* is not the origin. Upon applying the control policy \mathcal{F}_{v_t} by taking action u_t^* , we subsequently update the estimate of the variable vector according to iteration (8) where $\nabla_v V_{\mathcal{F}_v}$ is obtained from (7) of Theorem 4. In particular, the first partial derivative term on the right hand side of (7) is given by the standard policy gradient solution, and the second partial derivative term on the right hand side of (7) is obtained by differentiation of the CARE (6), which in turn renders (Kao and Hennequin, 2020)

$$dP \tilde{A}_v + \tilde{A}_v^\top dP + (dZ + dZ^\top + d\underline{Q}_v + K^\top dR_v K) = 0, \quad (9)$$

where $\tilde{A}_v = A_v - B_v K$ and $dZ = P(dA_v - dB_v K)$.

Our CBRL approach combined with the LQR control-theoretic framework concerns the linear dynamics $\dot{x} = A_v x + B_v u$ where A_v and B_v contain elements of the unknown independent-variable vector v . By leveraging known basic information about the LQR control problem at hand, only a relatively small number d of unknown variables need to be learned. For a wide range of applications where state variables are derivatives of each other w.r.t. time (e.g., position, velocity, acceleration, jerk), the corresponding rows in the A_v matrix consist of a single 1 and the corresponding rows in B_v comprise zeros. We exploit this basic information to consider general matrix forms for A_v and B_v that reduce the number of unknown variables to be learned. As a representative illustration, the system dynamics when there are two groups of such variables have the form given by (16) in Appendix A.5.

3. Experimental Results

In this section, we conduct numerical experiments to empirically evaluate the performance of our general CBRL approach combined with the LQR control-theoretic framework of Section 2, as summarized in Algorithm 1 of Appendix A.5. The objective (1) seeks to maximize the expected cumulative discounted reward, simply referred to as the expected return. Our numerical experiments consider several classical RL tasks from Gymnasium (Towers et al., 2023), including *Cart Pole*, *Lunar Lander (Continuous)*, *Mountain Car (Continuous)*, and *Pendulum*. We compare our CBRL method with three state-of-the-art RL algorithms, namely DQN (Mnih et al., 2013) for discrete actions, DDPG (Lillicrap et al., 2015) for continuous actions and PPO (Schulman et al., 2017), together with a variant of PPO that solely replaces the nonlinear policy of PPO with a linear policy (since we know the optimal policy for some of the problems, e.g., *Cart Pole*, is linear). These baselines are selected as the state-of-the-art algorithms for solving the RL tasks under consideration. Experimental details and additional results are provided in Appendix B both in general and for each RL task.

We have chosen the LQR control-theoretic framework to be combined as part of our CBRL approach with the understanding that not all of the above RL tasks can be adequately solved using LQR even if the variable vector v is known. Recall, however, that our CBRL approach allows the domain of the control policies to span a subset of states in \mathbb{X} , thus enabling partitioning of the state space so that properly increased richness w.r.t. finer and finer granularity can provide improved approximations and asymptotic optimality according to Theorem 3, analogous to the class of canonical piecewise-linear function approximations (Lin and Unbehauen, 1992). While *Cart Pole* and *Lunar Lander (Continuous)* can be directly addressed within the context of LQR, this is not the case for *Mountain Car (Continuous)* and *Pendulum* which require a nonlinear controller. We therefore partition the state space in the case of such RL tasks and consider a corresponding piecewise-LQR controller where the learned variable vectors may differ or be shared across the partitions.

All variables of our CBRL approach are randomly initialized uniformly within $(0, 1)$ and then learned using our control-policy-variable gradient ascent iteration (8). We consider four sets of initial variables to validate the robustness of our CBRL approach for each RL task (see Appendix B).

3.1. *Cart Pole* under CBRL LQR

Cart Pole, as depicted in Fig. 2 of Appendix B.1, consists of a pole connected to a horizontally moving cart with the goal of balancing the pole by applying a force on the cart to the left or right.

The state of the system is $x = [p, \dot{p}, \theta, \dot{\theta}]$ in terms of the position of the cart p , the velocity of the cart \dot{p} , the angle of the pole θ , and the angular velocity of the pole $\dot{\theta}$. With upright initialization of the pole on the cart, each episode comprises 200 steps and the problem is considered “solved” upon achieving an average return of 195.

The LQR controller can be used to solve the *Cart Pole* problem provided that all the variables of the system are known (e.g., mass of cart, mass and length of pole, gravity), where the angle is kept small by our CBRL approach combined with the LQR framework. We address the problem within the context of our CBRL approach by exploiting the general matrix form for the LQR dynamics given by (17) in Appendix B.1, solely taking into account general physical relationships (e.g., the derivative of the angle of the pole is equivalent to its angular velocity) and laws (e.g., the force can only affect the acceleration), with the $d = 10$ unknown variables $a_0, \dots, a_7, b_0, b_1$ to be learned; refer to Fig. 1(c).

Fig. 1(a) – 1(c) and Table 1 (Appendix B.1) present numerical results for the three state-of-the-art baselines (discrete actions) and our CBRL approach, with each run over five independent random seeds; see Table 2 and Fig. 3 in Appendix B.1 for the four sets of initial variables in (17). Fig. 1(a) – 1(b), Table 1 and Fig. 3(a) – 3(b) clearly demonstrate that our CBRL approach provides far superior performance (both mean and standard deviation) over all baselines w.r.t. both the number of episodes and running time, in addition to demonstrating a more stable training process. Fig. 3(c) – 3(f) illustrates the learning behavior of CBRL variables given different initialization.

3.2. Lunar Lander under CBRL LQR

Lunar Lander (Continuous), as depicted in Fig. 4 of Appendix B.2, is a classical spacecraft trajectory optimization problem with the goal to land softly and fuel-efficiently on a landing pad by applying thrusters to the left, to the right, and upward. The state of the system is $x = [p_x, v_x, p_y, v_y, \theta, \dot{\theta}]$ in terms of the (x, y) positions p_x and p_y , two linear velocities v_x and v_y , angle θ , and angular velocity $\dot{\theta}$. Starting at the top center of the viewport with a random initial force applied to its center of mass, the lander (spacecraft) is subject to gravity, friction and turbulence while surfaces on the “moon” are randomly generated in each episode with the target landing pad centered at $(0, 0)$. The problem is considered “solved” upon achieving an average return of 200.

The LQR controller can be used to solve the *Lunar Lander (Continuous)* problem provided that all variables of the system are known (e.g., mass of lander, gravity, friction, etc.), where the angle is kept small by our CBRL approach combined with the LQR framework. We address the problem within the context of our CBRL approach by exploiting the general matrix form for the LQR dynamics given by (18) in Appendix B.2, solely taking into account general physical relationships (akin to *Cart Pole*) and mild physical information from the system state (e.g., the acceleration is independent of the position), with the $d = 15$ unknown variables $a_0, \dots, a_{11}, b_0, b_1, b_2$ to be learned; refer to Fig. 1(f).

Fig. 1(d) – 1(f) and Table 3 (Appendix B.2) present numerical results for the three state-of-the-art baselines (continuous actions) and our CBRL approach, with each run over five independent random seeds; see Table 4 and Fig. 5 in Appendix B.2 for the four sets of initial variables in (18). Fig. 1(d) – 1(e), Table 3 and Fig. 5(a) – 5(b) clearly demonstrate that our CBRL approach provides far superior performance (both mean and standard deviation) over all baselines w.r.t. both the number of episodes and running time, in addition to demonstrating a more stable training process. We note that the baseline algorithms often crash and terminate sooner than the more successful landings

of our CBRL approach, resulting in the significantly worse performance exhibited in Fig. 1(d) – 1(e), Table 3 and Fig. 5. Finally, Fig. 5(c) – 5(f) illustrates the learning behavior of CBRL variables given different initialization.

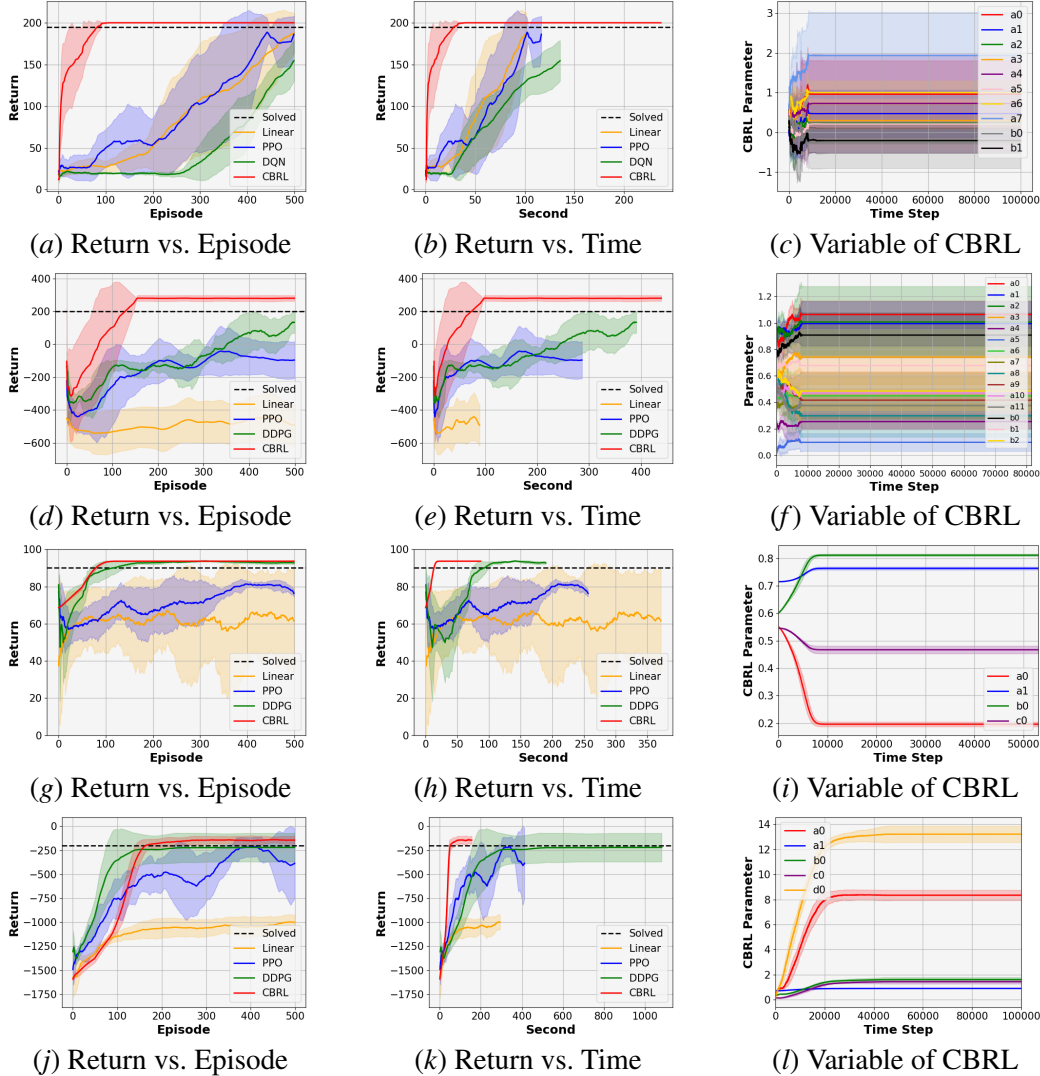


Figure 1: Learning curves over five independent runs comparing our CBRL approach with the Linear policy, PPO, DQN (discrete actions), and DDPG (continuous actions), where the solid line shows the mean and the shaded area depicts the standard deviation for CartPole (a)-(c), LunarLander (d)-(f), MountainCar (g)-(i), and Pendulum (j)-(l).

3.3. Mountain Car under CBRL Piecewise-LQR

Mountain Car (Continuous), as depicted in Fig. 6 of Appendix B.3, consists of the placement of a car in a valley with the goal of accelerating the car to reach the target at the top of the hill on the right by applying a force on the car to the left or right. The system state is $x = [p, v]$ in terms

of the position of the car p and the velocity of the car v . With random initialization at the bottom of the valley, the problem is considered “solved” upon achieving an average return of 90.

Recall that the LQR controller is not sufficient to solve the *Mountain Car (Continuous)* problem, even if all the variables of the system are known (e.g., mass of the car and gravity), because a nonlinear controller is required. Consequently, we consider a piecewise-LQR controller that partitions the state space into two regions (LQR 1 and LQR 2 in Fig. 6 of Appendix B.3). The target state $x^* = [p^*, v^*]$ is selected to be $x^* = [-1.2, 0]$ if $v < 0$ (LQR 1), and to be $x^* = [0.6, 0]$ otherwise (LQR 2), where -1.2 and 0.6 represent the position of the left hill and the right hill, respectively. We address the problem within the context of our CBRL approach by exploiting the general matrix form for the piecewise-LQR dynamics given by (19) in Appendix B.3, solely taking into account general physical relationships and laws, with the $d = 4$ unknown variables a_0, a_1, b_0, c_0 to be learned; refer to Fig. 1(i).

Fig. 1(g) – 1(i) and Table 5 (Appendix B.3) present numerical results for the three state-of-the-art baselines (continuous actions) and our CBRL approach, with each run over five independent random seeds; refer to Table 6 and Fig. 7 in Appendix B.3 for the four sets of initial variables in (19). Fig. 1(g) – 1(h), Table 5 and Fig. 7(a) – 7(b) clearly demonstrate that our CBRL approach provides superior performance (both mean and standard deviation) over all baselines w.r.t. both the number of episodes and running time, in addition to demonstrating a more stable training process. Fig. 7(c) – 7(f) illustrates the learning behavior of CBRL variables given different initialization.

3.4. *Pendulum* under CBRL Piecewise-LQR

Pendulum, as depicted in Fig. 8 of Appendix B.4, consists of a link attached at one end to a fixed point and the other end being free, with the goal of swinging up to an upright position by applying a torque on the free end. The state of the system is $x = [\theta, \dot{\theta}]$ in terms of the angle of the link θ and the angular velocity of the link $\dot{\theta}$. With random initial link position, each episode comprises 200 steps and the problem is considered “solved” upon achieving an average return of -200 .

Recall that the LQR controller is not sufficient to solve the *Pendulum* problem, even if all the variables of the system are known (e.g., mass of the link m , length of the link l , moment of inertia of the link J , and gravity g), because a nonlinear controller is required. Consequently, we consider a piecewise-LQR controller that partitions the state space into four regions (LQR 1 – 4 in Fig. 8 of Appendix B.4). In terms of the target state $x^* = [\theta^*, \dot{\theta}^*]$, the angle θ^* is selected based on the boundary angle in each partition (counter-clockwise boundary angle if $\dot{\theta} > 0$, and clockwise boundary angle otherwise), while the angular velocity $\dot{\theta}^*$ is selected based on the energy conservation law; see Appendix B.4 for more details. We address the problem within the context of our CBRL approach by exploiting the general matrix form for the piecewise-LQR dynamics given by (20) in Appendix B.4, solely taking into account general physical relationships and laws, with the $d = 5$ unknown variables a_0, a_1, b_0, c_0, d_0 to be learned; refer to Fig. 1(l).

Fig. 1(j) – 1(l) and Table 7 (Appendix B.4) present numerical results for the three state-of-the-art baselines (continuous actions) and our CBRL approach, with each run over five independent random seeds; see Table 8 and Fig. 9 in Appendix B.4 for the four sets of initial variables in (20). Fig. 1(j) – 1(k), Table 7 and Fig. 9(a) – 9(b) clearly demonstrate that our CBRL approach provides far superior performance (both mean and standard deviation) over all baselines w.r.t. the number of episodes upon convergence of our CBRL algorithm after a relatively small number of episodes and w.r.t. the running time across all episodes. In particular, even with only four partitions for the difficult

nonlinear *Pendulum* RL task, our CBRL approach provides significantly better mean performance and a much lower standard deviation than the closest competitor DDPG after around 150 episodes. Moreover, Fig. 1(k) clearly demonstrates that our CBRL approach outperforms all other baselines w.r.t. running time. These numerical results also demonstrate a more stable training process for our CBRL approach. Finally, Fig. 9(c) – 9(f) illustrates the learning behavior of CBRL variables given different initialization.

3.5. Discussion

Our numerical results demonstrate an important form of robustness exhibited by the optimal control policy of our CBRL approach w.r.t. the learned variable values. In particular, we performed additional comparative numerical experiments to evaluate the performance of LQR with the known true variables for *Cart Pole* and the performance of piecewise-LQR with the known true variables for *Mountain Car* and *Pendulum* (*Lunar Lander* is omitted because its underlying true variables are not known to us). We then compare the relative difference between these numerical results for LQR with the true variables and the corresponding numerical results of our CBRL approach in Fig. 1(a) – 1(b), Fig. 1(g) – 1(h), and Fig. 1(j) – 1(k). It is important to note that the variable values learned by our CBRL approach and presented in Fig. 1(c), Fig. 1(i), and Fig. 1(l) differ considerably from the corresponding true variables. Despite these non-negligible variable value differences, the comparative relative performance differences for *Cart Pole* and *Pendulum* respectively show that LQR and piecewise-LQR with the true variables provide no improvement in return over the corresponding return of our CBRL approach in Fig. 1(a) – 1(b) and Fig. 1(j) – 1(k). In addition, the return of our CBRL approach for *Mountain Car* in Fig. 1(g) – 1(h) is within 2% of the corresponding return of piecewise-LQR with the true variables.

The supremum over the variable space in the definition of our CBRL operator (3), together with its unique fixed point (4), and the Q -learning update rule (5) are primarily used for theoretical purposes in this paper. However, one might be concerned about potential computational challenges associated with the supremum when the variable space is continuous. We first note that this issue is not fundamentally different from the corresponding challenges in standard RL when the action space is continuous, and thus similar steps can be taken to address the issue. Another important factor that mitigates such concerns is the foregoing robustness of the optimal control policy w.r.t. the learned variable values. Lastly, we note that this issue did not arise in our numerical experiments using Algorithm 1.

One important implementation issue is stepsize selection, just like in nonconvex optimization and RL. We address this issue by using similar methods employed in standard RL, i.e., the adaptive stepsize selection in our implementation of Algorithm 1. Specifically, we reduce the stepsize η in (8) by a factor of 0.99 each time achieving the “solved” return. Another important implementation issue concerns variable-vector initialization, again like in nonconvex optimization and RL. As discussed for each of the above RL tasks, the numerical results in Figs. 3, 5, 7, 9 demonstrate the robustness of our CBRL approach w.r.t. variable-vector initialization. An additional important factor here is the aforementioned robustness of the optimal control policy w.r.t. the learned variable values. Moreover, given the efficiency of our CBRL approach relative to state-of-the-art methods, additional computations for stepsize selection and variable-vector initialization can be employed when issues are encountered while retaining overall computational efficiencies.

4. Conclusion

In this paper we devise a CBRL approach to support direct learning of the optimal policy. We establish various theoretical properties of our approach, including convergence and optimality of our CBRL operator and Q -learning, a new control-policy-variable gradient theorem, and a gradient ascent algorithm based on this theorem within the context of the LQR control-theoretic framework as a representative example. We then conduct numerical experiments to empirically evaluate the performance of our general CBRL approach on several classical RL tasks. These numerical results demonstrate the significant benefits of our CBRL approach over state-of-the-art methods in terms of improved quality and robustness of the solution and reduced sample complexity and running time.

References

- Alekh Agarwal, Sham M. Kakade, Jason D. Lee, and Gaurav Mahajan. On the theory of policy gradient methods: Optimality, approximation, and distribution shift. *Journal of Machine Learning Research*, 22(98):1–76, 2021. URL <http://jmlr.org/papers/v22/19-736.html>.
- Christopher G. Atkeson and Juan Carlos Santamaria. A comparison of direct and model-based reinforcement learning. In *Proc. International Conference on Robotics and Automation*, 1997.
- D.P. Bertsekas and J.N. Tsitsiklis. *Neuro-Dynamic Programming*. Athena Scientific, 1996.
- Weiqin Chen, Dharmashankar Subramanian, and Santiago Paternain. Probabilistic constraint for safety-critical reinforcement learning. *IEEE Transactions on Automatic Control*, 2024.
- M.P. Deisenroth and C.E. Rasmussen. PILCO: a model-based and data-efficient approach to policy search. In *Proc. International Conference on Machine Learning*, 2011.
- Kefan Dong, Yannis Flet-Berliac, Allen Nie, and Emma Brunskill. Model-based offline reinforcement learning with local misspecification. In *Proceedings of the AAAI Conference on Artificial Intelligence*, volume 37, pages 7423–7431, 2023.
- Jiaheng Feng, Mingxiao Feng, Haolin Song, Wengang Zhou, and Houqiang Li. Suf: Stabilized unconstrained fine-tuning for offline-to-online reinforcement learning. In *Proceedings of the AAAI Conference on Artificial Intelligence*, volume 38, pages 11961–11969, 2024.
- J. K. Hale and M. A. Cruz. Existence, uniqueness and continuous dependence for hereditary systems. *Annali di Matematica Pura ed Applicata*, 85:63–81, 1970. ISSN 0373-3114. doi: 10.1007/bf02413530.
- Tommi Jaakkola, Michael I. Jordan, and Satinder P. Singh. On the convergence of stochastic iterative dynamic programming algorithms. *Neural Computation*, 6:1185–1201, 1994.
- L. Kaelbling, M. Littman, and A. Moore. Reinforcement learning: A survey. *Journal of Artificial Intelligence Research*, 4:237–285, 1996.
- Ta-Chu Kao and Guillaume Hennequin. Automatic differentiation of Sylvester, Lyapunov, and algebraic Riccati equations. *ArXiv e-prints*, November 2020.

- Aviral Kumar, Aurick Zhou, George Tucker, and Sergey Levine. Conservative Q-learning for offline reinforcement learning. *Advances in Neural Information Processing Systems*, 33:1179–1191, 2020.
- Peter Lancaster and Leiba Rodman. *Algebraic Riccati Equations*. Clarendon Press, 1995.
- Timothy P Lillicrap, Jonathan J Hunt, Alexander Pritzel, Nicolas Heess, Tom Erez, Yuval Tassa, David Silver, and Daan Wierstra. Continuous control with deep reinforcement learning. *arXiv preprint arXiv:1509.02971*, 2015.
- J.-N. Lin and R. Unbehauen. Canonical piecewise-linear approximations. *IEEE Transactions on Circuits and Systems-I: Fundamental Theory and Applications*, 39(8):697–699, 1992. ISSN 1057-7122. doi: 10.1109/81.168933.
- Jeremy McMahan, Young Wu, Xiaojin Zhu, and Qiaomin Xie. Optimal attack and defense for reinforcement learning. In *Proceedings of the AAAI Conference on Artificial Intelligence*, volume 38, pages 14332–14340, 2024.
- D. Meger, J. Higuera, A. Xu, P. Giguere, and G. Dudek. Learning legged swimming gaits from experience. In *Proc. International Conference on Robotics and Automation*, 2015.
- V. Mnih, K. Kavukcuoglu, D. Silver, A. Graves, I. Antonoglou, D. Wierstra, and R. Riedmiller. Playing Atari with deep reinforcement learning. In *NIPS Workshop on Deep Learning*, 2013.
- Anusha Nagabandi, Gregory Kahn, Ronald S. Fearing, and Sergey Levine. Neural network dynamics for model-based deep reinforcement learning with model-free fine-tuning. In *IEEE International Conference on Robotics and Automation (ICRA)*, page 7559–7566, May 2018.
- Zhiyong Peng, Changlin Han, Yadong Liu, and Zongtan Zhou. Weighted policy constraints for offline reinforcement learning. In *Proceedings of the AAAI Conference on Artificial Intelligence*, volume 37, pages 9435–9443, 2023.
- Martin L. Puterman. *Markov Decision Processes: Discrete Stochastic Dynamic Programming*. John Wiley & Sons, 2005.
- J. Randlov and P. Alstrom. Learning to drive a bicycle using reinforcement learning and shaping. In *Proc. International Conference on Machine Learning*, 1998.
- S. Schaal. Learning from demonstration. *Advances in Neural Information Processing Systems*, 1997.
- J.G. Schneider. Exploiting model uncertainty estimates for safe dynamic control learning. *Advances in Neural Information Processing Systems*, 1997.
- John Schulman, Sergey Levine, Pieter Abbeel, Michael Jordan, and Philipp Moritz. Trust region policy optimization. In *International conference on machine learning*, pages 1889–1897. PMLR, 2015.
- John Schulman, Filip Wolski, Prafulla Dhariwal, Alec Radford, and Oleg Klimov. Proximal policy optimization algorithms. *arXiv preprint arXiv:1707.06347*, 2017.

- Kevin Shen. Multi-world model in continual reinforcement learning. In *Proceedings of the AAAI Conference on Artificial Intelligence*, volume 38, pages 23757–23759, 2024.
- Richard S. Sutton and Andrew G. Barto. *Reinforcement Learning: An Introduction*. The MIT Press, second edition, 2020.
- Richard S Sutton, David McAllester, Satinder Singh, and Yishay Mansour. Policy gradient methods for reinforcement learning with function approximation. In S. Solla, T. Leen, and K. Müller, editors, *Advances in Neural Information Processing Systems*, volume 12. MIT Press, 1999. URL https://proceedings.neurips.cc/paper_files/paper/1999/file/464d828b85b0bed98e80ade0a5c43b0f-Paper.pdf.
- Csaba Szepesvari. Algorithms for reinforcement learning. In *Synthesis Lectures on Artificial Intelligence and Machine Learning*, volume 4.1, pages 1–103. Morgan & Claypool, 2010.
- Mark Towers, Jordan K. Terry, Ariel Kwiatkowski, John U. Balis, Gianluca de Cola, Tristan Deleu, Manuel Goulão, Andreas Kallinteris, Arjun KG, Markus Krimmel, Rodrigo Perez-Vicente, Andrea Pierré, Sander Schulhoff, Jun Jet Tai, Andrew Tan Jin Shen, and Omar G. Younis. Gymnasium, March 2023. URL <https://zenodo.org/record/8127025>.
- John N. Tsitsiklis. Asynchronous stochastic approximation and Q-learning. *Machine Learning*, 16: 185–202, 1994.
- C. Watkins. *Learning from Delayed Rewards*. PhD thesis, University of Cambridge, Cambridge, U.K., 1989.
- Zhe Zhang and Xiaoyang Tan. An implicit trust region approach to behavior regularized offline reinforcement learning. In *Proceedings of the AAAI Conference on Artificial Intelligence*, volume 38, pages 16944–16952, 2024.
- Han Zheng, Xufang Luo, Pengfei Wei, Xuan Song, Dongsheng Li, and Jing Jiang. Adaptive policy learning for offline-to-online reinforcement learning. In *Proceedings of the AAAI Conference on Artificial Intelligence*, volume 37, pages 11372–11380, 2023.

Appendix A. Control-Based Reinforcement Learning Approach

In this appendix, we present the proofs of our main theoretical results together with additional results and technical details related to our CBRL approach combined with the LQR control-theoretic framework as presented in Section 2. We also provide the algorithmic details of our control-policy-variable gradient ascent method used for our numerical results of Section 3 and Appendix B.

A.1. Proof of Theorem 1.

Assumption 1. *There exist a policy function \mathcal{G} in the family \mathbb{F} and a unique variable vector v^* in the independent-variable set \mathbb{V} such that, for any state $x \in \mathbb{X}$, $\pi^*(x) = \mathcal{F}_{v^*}(x) = \mathcal{G}(v^*)(x)$.*

Theorem 1. *For any $\gamma \in (0, 1)$, the operator \mathbf{T} in (3) is a contraction in the supremum norm. Supposing Assumption 1 holds for the family of policy functions \mathbb{F} and its variable set \mathbb{V} , the contraction operator \mathbf{T} achieves the same asymptotically optimal outcome as that of the Bellman operator \mathcal{T}_B .*

Proof Recall that $\tilde{\Pi} \subseteq \Pi$ denotes the set of all stationary policies that are directly determined by the control-policy functions $\mathcal{G}(v)$ over all $v \in \mathbb{V}$. Then, for the operator \mathbf{T} defined on $\tilde{\mathcal{Q}}(\mathbb{X} \times \tilde{\Pi})$ in (3) and for any two functions $\tilde{q}_1(x, \mathcal{F}_v) \in \tilde{\mathcal{Q}}(\mathbb{X} \times \tilde{\Pi})$ and $\tilde{q}_2(x, \mathcal{F}_v) \in \tilde{\mathcal{Q}}(\mathbb{X} \times \tilde{\Pi})$ with $v \in \mathbb{V}$, we obtain

$$\begin{aligned}
 \|\mathbf{T}\tilde{q}_1 - \mathbf{T}\tilde{q}_2\|_\infty &\stackrel{(a)}{=} \sup_{x \in \mathbb{X}, v \in \mathbb{V}} \left| \sum_{y \in \mathbb{X}} \mathbb{P}(y | x, \mathcal{F}_v) \left[r(x, \mathcal{F}_v(x)) + \gamma \sup_{v_1 \in \mathbb{V}} \tilde{q}_1(y, \mathcal{F}_{v_1}) \right. \right. \\
 &\quad \left. \left. - r(x, \mathcal{F}_v(x)) - \gamma \sup_{v_2 \in \mathbb{V}} \tilde{q}_2(y, \mathcal{F}_{v_2}) \right] \right| \\
 &\stackrel{(b)}{=} \sup_{x \in \mathbb{X}, v \in \mathbb{V}} \gamma \left| \sum_{y \in \mathbb{X}} \mathbb{P}(y | x, \mathcal{F}_v) \left[\sup_{v_1 \in \mathbb{V}} \tilde{q}_1(y, \mathcal{F}_{v_1}) - \sup_{v_2 \in \mathbb{V}} \tilde{q}_2(y, \mathcal{F}_{v_2}) \right] \right| \\
 &\stackrel{(c)}{\leq} \sup_{x \in \mathbb{X}, v \in \mathbb{V}} \gamma \sum_{y \in \mathbb{X}} \mathbb{P}(y | x, \mathcal{F}_v) \left| \sup_{v_1 \in \mathbb{V}} \tilde{q}_1(y, \mathcal{F}_{v_1}) - \sup_{v_2 \in \mathbb{V}} \tilde{q}_2(y, \mathcal{F}_{v_2}) \right| \\
 &\stackrel{(d)}{\leq} \sup_{x \in \mathbb{X}, v \in \mathbb{V}} \gamma \sum_{y \in \mathbb{X}} \mathbb{P}(y | x, \mathcal{F}_v) \sup_{z \in \mathbb{X}, v' \in \mathbb{V}} |\tilde{q}_1(z, \mathcal{F}_{v'}) - \tilde{q}_2(z, \mathcal{F}_{v'})| \\
 &\stackrel{(e)}{\leq} \sup_{x \in \mathbb{X}, v \in \mathbb{V}} \gamma \sum_{y \in \mathbb{X}} \mathbb{P}(y | x, \mathcal{F}_v) \|\tilde{q}_1 - \tilde{q}_2\|_\infty \\
 &\stackrel{(f)}{=} \gamma \|\tilde{q}_1 - \tilde{q}_2\|_\infty,
 \end{aligned}$$

where (a) is by definition in (3) noting that taking the supremum over \mathbb{V} is equivalent to taking the supremum over $\tilde{\Pi}$, (b) follows from straightforward algebra, (c) and (d) are due to the triangle inequality, and (e) and (f) directly follow by definition. For any $\gamma \in (0, 1)$, this establishes that the operator \mathbf{T} in (3) is a contraction in the supremum norm, thus rendering the desired result for the first part of the theorem.

For the second part of the theorem, under the stated supposition, we know that the optimal policy $\pi^*(x)$ realized by the Bellman operator holds for a unique vector v^* in the variable set \mathbb{V} and any $x \in \mathbb{X}$. We also know that the Bellman operator \mathcal{T}_B in (2) and our CBRL operator \mathbf{T} in (3)

are both contractions in supremum norm with unique fixed points, where the fixed point of the Bellman operator is the optimal solution of the Bellman equation. In particular, repeatedly applying the Bellman operator \mathcal{T}_B in (2) to an action-value function $q(x, u) \in \mathbb{Q}(\mathbb{X} \times \mathbb{U})$ is well-known to asymptotically yield the unique fixed point equation $\mathcal{T}_B q_B^* = q_B^*$ where

$$\begin{aligned} q_B^*(x, \pi^*(x)) &= \sum_{y \in \mathbb{X}} \mathbb{P}(y | x, \pi^*) \left[r(x, \pi^*(x)) + \gamma \sup_{u' \in \mathbb{U}} q_B^*(y, u') \right] \\ &= \sum_{y \in \mathbb{X}} \mathbb{P}(y | x, \pi^*) \left[r(x, \pi^*(x)) + \gamma q_B^*(y, \pi^*(y)) \right], \end{aligned} \quad (10)$$

with the second equality following from the definition of $\pi^*(x)$, and q_B^* is the optimal action-value function (Szepesvari, 2010). Likewise, repeatedly applying our CBRL operator \mathbf{T} in (3) to an action-value function $\tilde{q}(x, \mathcal{F}_v) \in \tilde{\mathbb{Q}}(\mathbb{X} \times \tilde{\Pi})$ asymptotically renders the unique fixed point equation $\mathbf{T} \tilde{q}_C^* = \tilde{q}_C^*$ where

$$\begin{aligned} \tilde{q}_C^*(x, \mathcal{F}_{v^*}) &= \sum_{y \in \mathbb{X}} \mathbb{P}(y | x, \mathcal{F}_{v^*}) \left[r(x, \mathcal{F}_{v^*}(x)) + \gamma \sup_{v' \in \mathbb{V}} \tilde{q}_C^*(y, \mathcal{F}_{v'}) \right] \\ &= \sum_{y \in \mathbb{X}} \mathbb{P}(y | x, \mathcal{F}_{v^*}) \left[r(x, \mathcal{F}_{v^*}(x)) + \gamma \tilde{q}_C^*(y, \mathcal{F}_{v^*}) \right], \end{aligned} \quad (11)$$

with the second equality following from the relationship between $\tilde{q}(x, \mathcal{F}_{v^*})$ and $\tilde{q}(x, \pi^*)$, given below in (12), under the supposition of the theorem together with the optimality of π^* . By showing that these two fixed points $q_B^*(x, \pi^*(x))$ and $\tilde{q}_C^*(x, \mathcal{F}_{v^*})$ in (10) and (11) coincide, the desired result follows.

To this end, from the definition of $\tilde{q}(x, \mathcal{F}_{v^*})$ and under the stated supposition of the theorem, we have for any $\tilde{q}(x, \mathcal{F}_{v^*}) \in \tilde{\mathbb{Q}}(\mathbb{X} \times \tilde{\Pi})$ and any $x \in \mathbb{X}$

$$\tilde{q}(x, \mathcal{F}_{v^*}) := q(x, \mathcal{F}_{v^*}(x)) = q(x, \pi^*(x)) =: \tilde{q}(x, \pi^*), \quad (12)$$

noting that v^* is the unique vector in the variable set \mathbb{V} associated with $\pi^*(x)$. Let $q_C^*(x, \mathcal{F}_{v^*}(x)) = \tilde{q}_C^*(x, \mathcal{F}_{v^*})$ denote the action-value function that corresponds by definition to $\tilde{q}_C^*(x, \mathcal{F}_{v^*})$ of (12) in accordance with (11). Then, in one direction to show $\tilde{q}_C^*(x, \mathcal{F}_{v^*}) \leq q_B^*(x, \pi^*(x))$, we derive

$$\begin{aligned} q_B^*(x, \pi^*(x)) &\stackrel{(a)}{=} \sum_{y \in \mathbb{X}} \mathbb{P}(y | x, \pi^*) \left[r(x, \pi^*(x)) + \gamma q_B^*(y, \pi^*(y)) \right] \\ &\stackrel{(b)}{\geq} \sum_{y \in \mathbb{X}} \mathbb{P}(y | x, \pi^*) \left[r(x, \pi^*(x)) + \gamma q_C^*(y, \pi^*(y)) \right] \\ &\stackrel{(c)}{=} \sum_{y \in \mathbb{X}} \mathbb{P}(y | x, \mathcal{F}_{v^*}) \left[r(x, \mathcal{F}_{v^*}(x)) + \gamma q_C^*(y, \mathcal{F}_{v^*}(y)) \right] \\ &\stackrel{(d)}{=} \sum_{y \in \mathbb{X}} \mathbb{P}(y | x, \mathcal{F}_{v^*}) \left[r(x, \mathcal{F}_{v^*}(x)) + \gamma \tilde{q}_C^*(y, \mathcal{F}_{v^*}) \right] \stackrel{(e)}{=} \tilde{q}_C^*(x, \mathcal{F}_{v^*}), \end{aligned} \quad (13)$$

where: (a) is directly from the definition of the fixed point in (10); (b) follows from the definition of the Bellman operator \mathcal{T}_B for any action-value function $q(x, u) \in \mathbb{Q}(\mathbb{X} \times \mathbb{U})$, the unique fixed

point (10), and the optimality of q_B^* and π^* ; (c) follows upon the substitution of policy \mathcal{F}_{v^*} for π^* and $q_C^*(x, \pi^*(x)) = q_C^*(x, \mathcal{F}_{v^*}(x))$ from (12); (d) follows upon the substitution of $q_C^*(x, \mathcal{F}_{v^*}(x)) = \tilde{q}_C^*(x, \mathcal{F}_{v^*})$ from (12); and (e) follows from (11). In the other direction to show $q_B^*(x, \pi^*(x)) \leq \tilde{q}_C^*(x, \mathcal{F}_{v^*})$, we derive

$$\begin{aligned}
 \tilde{q}_C^*(x, \mathcal{F}_{v^*}) &\stackrel{(a)}{=} \sum_{y \in \mathbb{X}} \mathbb{P}(y | x, \mathcal{F}_{v^*}) \left[r(x, \mathcal{F}_{v^*}(x)) + \gamma \tilde{q}_C^*(y, \mathcal{F}_{v^*}) \right] \\
 &\stackrel{(b)}{=} \sum_{y \in \mathbb{X}} \mathbb{P}(y | x, \mathcal{F}_{v^*}) \left[r(x, \mathcal{F}_{v^*}(x)) + \gamma q_C^*(y, \mathcal{F}_{v^*}(y)) \right] \\
 &\stackrel{(c)}{\geq} \sum_{y \in \mathbb{X}} \mathbb{P}(y | x, \mathcal{F}_{v^*}) \left[r(x, \mathcal{F}_{v^*}(x)) + \gamma q_B^*(y, \mathcal{F}_{v^*}(y)) \right] \\
 &\stackrel{(d)}{=} \sum_{y \in \mathbb{X}} \mathbb{P}(y | x, \pi^*) \left[r(x, \pi^*(x)) + \gamma q_B^*(y, \pi^*(y)) \right] \\
 &\stackrel{(e)}{=} q_B^*(x, \pi^*(x)), \tag{14}
 \end{aligned}$$

where: (a) is directly from the definition of the fixed point in (11); (b) follows upon the substitution of $q_C^*(x, \mathcal{F}_{v^*}(x)) = \tilde{q}_C^*(x, \mathcal{F}_{v^*})$ from (12); (c) follows from the definition of the CBRL operator \mathbf{T} for any action-value function $q(x, u) \in \mathbb{Q}(\mathbb{X} \times \mathbb{U})$, the unique fixed point (11), and the application of the Bellman optimality conditions on \tilde{q}_C^* in (11) for \mathcal{F}_{v^*} , all under the supposition of the theorem; (d) follows upon the substitution of policy π^* for \mathcal{F}_{v^*} and $q_B^*(x, \mathcal{F}_{v^*}(x)) = q_B^*(x, \pi^*(x))$ from (12); and (e) follows from (10). We therefore have coincidence of the fixed points (10) and (11), thus completing the proof. \blacksquare

A.2. Proof of Theorem 2.

Theorem 2. *Suppose Assumption 1 holds for the family of policy functions \mathbb{F} and its independent-variable set \mathbb{V} with a contraction operator \mathbf{T} as defined in (3). If $\sum_t \alpha_t = \infty$, $\sum_t \alpha_t^2 < \infty$, and r_t are bounded, then \tilde{q}_t under the Q-learning update rule (5) converges to the optimal fixed point \tilde{q}^* as $t \rightarrow \infty$ and the optimal policy function is obtained from a unique variable vector $v^* \in \mathbb{V}$.*

Proof We first rewrite (5) as a convex combination of

$$\tilde{q}_t(x_t, \mathcal{F}_{v,t}) \quad \text{and} \quad r_t + \gamma \sup_{v' \in \mathbb{V}} \tilde{q}_t(x_{t+1}, \mathcal{F}_{v'}),$$

where

$$\tilde{q}_{t+1}(x_t, \mathcal{F}_{v,t}) = (1 - \alpha_t(x_t, \mathcal{F}_{v,t})) \tilde{q}_t(x_t, \mathcal{F}_{v,t}) + \alpha_t(x_t, \mathcal{F}_{v,t}) \left[r_t + \gamma \sup_{v' \in \mathbb{V}} \tilde{q}_t(x_{t+1}, \mathcal{F}_{v'}) \right].$$

Define $\Delta_t := \tilde{q}_t - \tilde{q}^*$ to be the difference between \tilde{q}_t and \tilde{q}^* , which satisfies

$$\Delta_{t+1}(x_t, \mathcal{F}_{v,t}) = (1 - \alpha_t(x_t, \mathcal{F}_{v,t})) \Delta_t(x_t, \mathcal{F}_{v,t}) + \alpha_t(x_t, \mathcal{F}_{v,t}) \left[r_t + \gamma \sup_{v' \in \mathbb{V}} \tilde{q}_t(x_{t+1}, \mathcal{F}_{v'}) - \tilde{q}^* \right].$$

Further define

$$H_t(x, \mathcal{F}_v) := r(x, \mathcal{F}_v(x)) + \gamma \sup_{v' \in \mathbb{V}} \tilde{q}_t(X(x, \mathcal{F}_v), \mathcal{F}_{v'}) - \tilde{q}^*(x, \mathcal{F}_v),$$

where $X(x, \mathcal{F}_v)$ is a randomly sampled state from the MDP under an initial state x and policy \mathcal{F}_v . We then derive

$$\begin{aligned} \mathbb{E}[H_t(x, \mathcal{F}_v)|P_t] &= \sum_{y \in \mathbb{X}} \mathbb{P}(y|x, \mathcal{F}_v) \left[r(x, \mathcal{F}_v(x)) + \gamma \sup_{v' \in \mathbb{V}} \tilde{q}_t(y, \mathcal{F}_{v'}) - \tilde{q}^*(x, \mathcal{F}_v) \right] \\ &= (\mathbf{T}\tilde{q}_t)(x, \mathcal{F}_v) - \tilde{q}^*(x, \mathcal{F}_v) = (\mathbf{T}\tilde{q}_t)(x, \mathcal{F}_v) - (\mathbf{T}\tilde{q}^*)(x, \mathcal{F}_v), \end{aligned}$$

where $P_t = \{\Delta_t, \Delta_{t-1}, \dots, H_{t-1}, \dots, \alpha_{t-1}, \dots\}$ represents the past history of the process (Jaakkola et al., 1994; Tsitsiklis, 1994), and the last equality follows from $\tilde{q}^*(x, \mathcal{F}_v) = (\mathbf{T}\tilde{q}^*)(x, \mathcal{F}_v)$. From this equation together with Theorem 1, we conclude

$$\|\mathbb{E}[H_t(x, \mathcal{F}_v)|P_t]\|_\infty = \|\mathbf{T}\tilde{q}_t - \mathbf{T}\tilde{q}^*\|_\infty \leq \gamma \|\tilde{q}_t - \tilde{q}^*\|_\infty = \gamma \|\Delta_t\|_\infty.$$

Similarly, we derive

$$\begin{aligned} \text{Var}[H_t(x, \mathcal{F}_v)|P_t] &= \mathbb{E} \left[\left(r(x, \mathcal{F}_v(x)) + \gamma \sup_{v' \in \mathbb{V}} \tilde{q}_t(X(x, \mathcal{F}_v), \mathcal{F}_{v'}) - \tilde{q}^*(x, \mathcal{F}_v) \right. \right. \\ &\quad \left. \left. - (\mathbf{T}\tilde{q}_t)(x, \mathcal{F}_v) + \tilde{q}^*(x, \mathcal{F}_v) \right)^2 \right] \\ &= \mathbb{E} \left[\left(r(x, \mathcal{F}_v(x)) + \gamma \sup_{v' \in \mathbb{V}} \tilde{q}_t(X(x, \mathcal{F}_v), \mathcal{F}_{v'}) - (\mathbf{T}\tilde{q}_t)(x, \mathcal{F}_v) \right)^2 \right] \\ &= \text{Var} \left[r(x, \mathcal{F}_v(x)) + \gamma \sup_{v' \in \mathbb{V}} \tilde{q}_t(X(x, \mathcal{F}_v), \mathcal{F}_{v'}) \middle| P_t \right] \\ &\leq \kappa(1 + \|\Delta_t\|_\infty^2), \quad \text{for some } \kappa > 0, \end{aligned}$$

where the inequality follows from $r(\cdot, \cdot)$ being bounded.

The desired result for the convergence of the Q -learning algorithm to the optimal fixed point then follows from (Tsitsiklis, 1994, Theorem 3), (Jaakkola et al., 1994, Theorem 1). Finally, as a consequence of Assumption 1, we conclude that the optimal policy function is obtained from a unique variable vector $v^* \in \mathbb{V}$, thus completing the proof. \blacksquare

A.3. Proof of Theorem 3.

Suppose \mathbb{F} satisfies Assumption 1, and consider a sequence of less rich families $\mathbb{F}_1, \dots, \mathbb{F}_k$ of policy functions $\mathcal{G}^{(i)} \in \mathbb{F}_i$ obtained from independent-variable vectors of the corresponding independent variable sets \mathbb{V}_i , further defining the operators $\mathbf{T}_i : \tilde{\mathbb{Q}}(\mathbb{X} \times \tilde{\Pi}_i) \rightarrow \tilde{\mathbb{Q}}(\mathbb{X} \times \tilde{\Pi}_i)$ as in (3) for any function $\tilde{q}_i(x, \mathcal{F}_v^{(i)}) \in \tilde{\mathbb{Q}}(\mathbb{X} \times \tilde{\Pi}_i)$, $i \in [k] := \{1, \dots, k\}$. From Theorem 1, for $i \in [k]$, we have that the contraction operators $\mathbf{T}_i : \mathbb{Q}(\mathbb{X} \times \tilde{\Pi}_i) \rightarrow \mathbb{Q}(\mathbb{X} \times \tilde{\Pi}_i)$ under the variable sets \mathbb{V}_i converge to the unique fixed points $\tilde{q}_i^*(x, \mathcal{F}_v^{(i)})$ which satisfy, for all $x \in \mathbb{X}$ and $v \in \mathbb{V}_i$,

$$\tilde{q}_i^*(x, \mathcal{F}_v^{(i)}) = \sum_{y \in \mathbb{X}} \mathbb{P}(y|x, \mathcal{F}_v^{(i)}) \left[r(x, \mathcal{F}_v^{(i)}(x)) + \gamma \sup_{v' \in \mathbb{V}_i} \tilde{q}_i^*(y, \mathcal{F}_{v'}^{(i)}) \right] \quad (15)$$

corresponding to (4). Let us first consider two such families \mathbb{F}_1 and \mathbb{F}_2 , for which we introduce the following lemma used in the proof of Theorem 3.

Lemma 5 *Assume the state and action spaces are compact and \mathcal{F}_v is uniformly continuous for each v . For two variable sets \mathbb{V}_1 and \mathbb{V}_2 and any two variable vectors $v_1 \in \mathbb{V}_1$ and $v_2 \in \mathbb{V}_2$, let $d(\cdot, \cdot)$ be a sup-norm distance function defined over the policy space $\tilde{\Pi}$, i.e., $d(\mathcal{F}_{v_1}^{(1)}, \mathcal{F}_{v_2}^{(2)}) = \sup_{x \in \mathbb{X}} \|\mathcal{F}_{v_1}^{(1)}(x) - \mathcal{F}_{v_2}^{(2)}(x)\|$. Then, for all $\epsilon > 0$ there exists $\delta > 0$ such that, if for all $v_1 \in \mathbb{V}_1$ there exists $v_2 \in \mathbb{V}_2$ with $d(\mathcal{F}_{v_1}^{(1)}, \mathcal{F}_{v_2}^{(2)}) < \delta$ and if for all $v_2 \in \mathbb{V}_2$ there exists $v_1 \in \mathbb{V}_1$ with $d(\mathcal{F}_{v_1}^{(1)}, \mathcal{F}_{v_2}^{(2)}) < \delta$, we have $\sup_{x \in \mathbb{X}} \|\tilde{q}_1^* - \tilde{q}_2^*\| < \epsilon$.*

Proof Since the state and action spaces are compact and \mathcal{F}_v is uniformly continuous for each v , it then follows from Lemma 2.2 in Hale and Cruz (1970) that the unique fixed point depends continuously on the contraction mapping \mathbf{T} and thus we find that \tilde{q}^* w.r.t. its second argument depends continuously on the sets \mathbb{V}_i , which implies the desired result. \blacksquare

Intuitively, Lemma 5 shows that, for any policy families \mathbb{F}_1 and \mathbb{F}_2 sufficiently close to each other, the fixed points \tilde{q}_1 and \tilde{q}_2 of the corresponding operators \mathbf{T}_1 and \mathbf{T}_2 are also close to each other. When the policy family \mathbb{F}_k is sufficiently rich and approaches \mathbb{F} , then the fixed point of the corresponding operator \mathbf{T}_k approaches the unique fixed point of \mathbb{F} satisfying (4), and therefore they approach the optimal q -value as promised by Bellman from Theorem 1. We formally characterize this asymptotic convergence of approximate optimality to global optimality in Theorem 3.

Theorem 3. *Assume the state and action spaces are compact and \mathcal{F}_v is uniformly continuous for each v . Consider \mathbb{F} and a sequence of families of policy functions $\mathbb{F}_1, \mathbb{F}_2, \dots, \mathbb{F}_{k-1}, \mathbb{F}_k$, with \mathbb{V} and \mathbb{V}_i respectively denoting the independent-variable sets corresponding to \mathbb{F} and \mathbb{F}_i , $i \in [k]$. Let $d(\cdot, \cdot)$ be a sup-norm distance function defined over the policy space $\tilde{\Pi}$, i.e., $d(\mathcal{F}_{v_i}^{(i)}, \mathcal{F}_{v_j}^{(j)}) = \sup_{x \in \mathbb{X}} \|\mathcal{F}_{v_i}^{(i)}(x) - \mathcal{F}_{v_j}^{(j)}(x)\|$, $v_i \in \mathbb{V}_i, v_j \in \mathbb{V}_j$. Further let $d'(\cdot, \cdot)$ be an inf-norm distance function defined over the policy function space \mathbb{F} , i.e., $d'(\mathcal{G}^{(i)}, \mathcal{G}^{(j)}) = \inf_{v_i \in \mathbb{V}_i, v_j \in \mathbb{V}_j} d(\mathcal{G}^{(i)}(v_i), \mathcal{G}^{(j)}(v_j))$, $\mathcal{G}^{(i)} \in \mathbb{F}_i, \mathcal{G}^{(j)} \in \mathbb{F}_j$. Suppose, for all $\mathcal{G} \in \mathbb{F}$, there exists a $\mathcal{G}^{(k)} \in \mathbb{F}_k$ such that $d'(\mathcal{G}^{(k)}, \mathcal{G}) \rightarrow 0$ as $k \rightarrow \infty$. Then, $\|\tilde{q}_k^* - \tilde{q}^*\|_\infty \rightarrow 0$ as $k \rightarrow \infty$.*

Proof First, in the definition of the contraction mapping \mathbf{T} , the result of the supremum depends continuously on the set \mathbb{V} and thus the corresponding argument of \mathbf{T} depends continuously on \mathbb{V} . The desired result then follows from Lemma 5. \blacksquare

A.4. Proof of Theorem 4.

Theorem 4. *Consider a family of control policy functions \mathbb{F} , its independent-variable set \mathbb{V} with contraction operator \mathbf{T} in the form of (3), and the value function $V_{\mathcal{F}_v}$ under the control policy \mathcal{F}_v . Assuming $\mathcal{F}_{v,u}(x)$ is differentiable w.r.t. \mathcal{F}_v and $\mathcal{F}_v(x)$ is differentiable w.r.t. v (i.e., both $\partial \mathcal{F}_{v,u}(x) / \partial \mathcal{F}_v$ and $\partial \mathcal{F}_v(x) / \partial v$ exist), we then have*

$$\nabla_v V_{\mathcal{F}_v}(x_0) = \sum_{x \in \mathbb{X}} \sum_{k=0}^{\infty} \gamma^k \mathbb{P}(x, k | x_0, \mathcal{F}_v) \left[\sum_{u \in \mathbb{U}} \frac{\partial \mathcal{F}_{v,u}(x)}{\partial \mathcal{F}_v} \frac{\partial \mathcal{F}_v(x)}{\partial v} \tilde{q}_u(x, \mathcal{F}_v) \right]. \quad (7)$$

Proof We derive

$$\begin{aligned}
 \nabla_v V_{\mathcal{F}_v}(x_0) &\stackrel{(a)}{=} \nabla_v \left[\sum_u \mathcal{F}_{v,u}(x_0) \tilde{q}_u(x_0, \mathcal{F}_v) \right] \\
 &\stackrel{(b)}{=} \sum_u [\nabla_v \mathcal{F}_{v,u}(x_0) \tilde{q}_u(x_0, \mathcal{F}_v) + \mathcal{F}_{v,u}(x_0) \nabla_v \tilde{q}_u(x_0, \mathcal{F}_v)] \\
 &\stackrel{(c)}{=} \sum_u \left[\nabla_v \mathcal{F}_{v,u}(x_0) \tilde{q}_u(x_0, \mathcal{F}_v) + \mathcal{F}_{v,u}(x_0) \nabla_v \sum_{x,r} \mathbb{P}(x, r | x_0, \mathcal{F}_v, u) (r + \gamma V_{\mathcal{F}_v}(x)) \right] \\
 &\stackrel{(d)}{=} \sum_u \left[\nabla_v \mathcal{F}_{v,u}(x_0) \tilde{q}_u(x_0, \mathcal{F}_v) + \gamma \mathcal{F}_{v,u}(x_0) \sum_x \mathbb{P}(x | x_0, \mathcal{F}_v, u) \nabla_v V_{\mathcal{F}_v}(x) \right] \\
 &\stackrel{(e)}{=} \sum_u \left[\nabla_v \mathcal{F}_{v,u}(x_0) \tilde{q}_u(x_0, \mathcal{F}_v) + \gamma \mathcal{F}_{v,u}(x_0) \sum_x \mathbb{P}(x | x_0, \mathcal{F}_v, u) \sum_{u'} \left[\nabla_v \mathcal{F}_{v,u'}(x) \tilde{q}_{u'}(x, \mathcal{F}_v) \right. \right. \\
 &\qquad \qquad \qquad \left. \left. + \gamma \mathcal{F}_{v,u'}(x) \sum_{x'} \mathbb{P}(x' | x, \mathcal{F}_v, u') \nabla_v V_{\mathcal{F}_v}(x') \right] \right] \\
 &\stackrel{(f)}{=} \sum_{x \in \mathbb{X}} \sum_{k=0}^{\infty} \gamma^k \mathbb{P}(x, k | x_0, \mathcal{F}_v) \sum_u \nabla_v \mathcal{F}_{v,u}(x) \tilde{q}_u(x, \mathcal{F}_v),
 \end{aligned}$$

where (a) is by the definition of the value function for state x_0 , (b) follows from the product rule, (c) follows by the definition of $\tilde{q}_u(x, \mathcal{F}_v)$, (d) follows by applying the gradient w.r.t. v summed over all r , (e) follows by repeating each of the preceding steps for $\nabla_v V_{\mathcal{F}_v}(x')$, and (f) follows from repeated unrolling along the lines of (e) and upon recalling $\mathbb{P}(x, k | x_0, \mathcal{F}_v)$ to be the probability of going from state x_0 to state x in k steps under the control policy \mathcal{F}_v .

The result then follows since $\nabla_v \mathcal{F}_{v,u}(x) = \frac{\partial \mathcal{F}_{v,u}(x)}{\partial \mathcal{F}_v} \frac{\partial \mathcal{F}_v(x)}{\partial v}$, by the chain rule. \blacksquare

A.5. Control-Policy-Variable Gradient Ascent Algorithm

Based on our new CBRL gradient theorem (Theorem 4), we devise control-policy-variable gradient ascent methods within the context of our general CBRL approach. One such gradient ascent method for directly learning the unknown variable vector v of the optimal control policy w.r.t. the value function V comprises the iterative process according to (8) with stepsize η . Here $\nabla_v V_{\mathcal{F}_v}$ is as given by (7), where the first gradient term $\partial \mathcal{F}_{v,u}(x) / \partial \mathcal{F}_v$ is essentially the standard policy gradient, and the second gradient term $\partial \mathcal{F}_v(x) / \partial v$ is specific to the control-theoretic framework employed in our general CBRL approach; refer to Section 2 regarding the LQR control-theoretic framework combined as part of our CBRL approach. We note that standard policy gradient ascent methods are a special case of (8) where the independent-variable vector v is directly replaced by the policy π . In particular, the special case of \mathcal{G} being an identity map and $\frac{\partial V}{\partial \mathcal{F}_{v_t}} \frac{\partial \mathcal{F}_{v_t}}{\partial v_t}$ replaced by $\frac{\partial V}{\partial \pi_t}$ corresponds to the direct policy gradient parameterization case in Agarwal et al. (2021).

Our algorithmic implementation of the above control-policy-variable gradient ascent method is summarized in Algorithm 1. This algorithm, together with our general CBRL approach combined with the LQR control-theoretic framework as presented in Section 2, is used to obtain the numerical results for our CBRL approach presented in Section 3 and Appendix B.

Algorithm 1 Control-Policy-Variable Gradient Ascent Algorithm

Require: $\mathcal{E}, \mathbb{X}, \mathbb{U}, \mathbb{F}, \mathcal{F}_v, \mathbf{u}(\cdot, \cdot), D_0 = \Phi, \eta, N$ \triangleright Environment, State Set, Control Action Set, Control-Policy Family, Control-Policy, Control Action Generator (CBRL-LQR), Empty Rollout Dataset, Stepsize, Number of Iterations

Initialize $v_0 \mid \mathcal{F}_{v_0} \in \mathbb{F}, \mathbf{X}_0 \in \mathbb{X}$

for $t = 0, 1, \dots, N$ **do**

1. Generate the control action given the current state and control-policy-variable

$$\mathbf{u}_t = \mathbf{u}(\mathbf{X}_t, v_t)$$

2. Collect the rollout transition data by applying the control action to the environment \mathcal{E}

$$\mathcal{E} \xrightarrow{\mathbf{u}_t} \text{rollout} := (\mathbf{X}_t, \mathbf{u}_t, r, \mathbf{X}_{t+1})$$

$$D_{t+1} = D_t \cup \text{rollout}$$

3. Compute the control-policy-variable gradient (7) by using the standard policy gradient solution for the first partial derivative and (9) for the second partial derivative, given the current rollout dataset D_{t+1}
4. Update the control-policy-variable using the gradient ascent iteration (8)

$$v_{t+1} = v_t + \eta \nabla_v V_{\mathcal{F}_v}(\mathbf{X}_t)$$

Our CBRL approach combined with the LQR control-theoretic framework concerns the linear dynamics $\dot{x} = A_v x + B_v u$ where A_v and B_v contain elements of the unknown variable vector v . By leveraging known basic information about the LQR control problem at hand, only a relatively small number d of unknown variables need to be learned. For a wide range of applications where state variables are derivatives of each other w.r.t. time (e.g., position, velocity, acceleration, jerk), the corresponding rows in the A_v matrix consist of a single 1 and the corresponding rows in B_v comprise zeros. We exploit this basic information to consider general matrix forms for A_v and B_v that reduce the number of unknown variables to be learned. As a representative illustration, the system dynamics when there are two groups of such variables have the form given by

$$\underbrace{\begin{bmatrix} \frac{dx_1}{dt} \\ \vdots \\ \frac{d^{k_1} x_1}{dt^{k_1}} \\ \frac{dx_2}{dt} \\ \vdots \\ \frac{d^{k_2} x_2}{dt^{k_2}} \end{bmatrix}}_{\dot{x}} = \underbrace{\begin{bmatrix} 0 & 1 & 0 & \dots & & 0 \\ 0 & 0 & 1 & \dots & & \\ a_{10} & \dots & & & & a_{1n} \\ 0 & \dots & & 0 & 1 & \dots & 0 \\ 0 & \dots & & & 0 & 1 & \dots \\ a_{20} & \dots & & & & & a_{2n} \end{bmatrix}}_{A_v} x + \underbrace{\begin{bmatrix} 0 \\ \vdots \\ b_0 \\ 0 \\ \vdots \\ b_1 \end{bmatrix}}_{B_v} u. \quad (16)$$

Appendix B. Experimental Results

In this appendix we provide additional details and results w.r.t. our numerical experiments to evaluate the performance of our general CBRL approach combined with the LQR control-theoretic framework as presented in Section 2 and using Algorithm 1. Recall that we consider the following classical RL tasks from Gymnasium (Towers et al., 2023): *Cart Pole*, *Lunar Lander (Continuous)*, *Mountain Car (Continuous)*, and *Pendulum*. Our CBRL approach is compared against the three state-of-the-art RL algorithms DQN (Mnih et al., 2013) for discrete actions, DDPG (Lillicrap et al., 2015) for continuous actions and PPO (Schulman et al., 2017), together with a variant of PPO that solely replaces the nonlinear policy of PPO with a linear policy (since we know the optimal policy for problems such as *Cart Pole* is linear). These baselines are selected as the state-of-the-art RL algorithms for solving the RL tasks under consideration.

Our CBRL approach depends in part upon the control-theoretic framework with which it is combined, where we have chosen LQR as a representative example with the understanding that not all of the above RL tasks can be adequately solved using LQR even if the variable vector v is known. Recall, however, that our CBRL approach allows the domain of the control policies to span a subset of states in \mathbb{X} , thus enabling the partitioning of the state space so that properly increased richness w.r.t. finer and finer granularity can provide improved approximations and asymptotic optimality according to Theorem 3 of Section 2, analogous to the class of canonical piecewise-linear function approximations (Lin and Unbehauen, 1992). While *Cart Pole* and *Lunar Lander (Continuous)* can be directly addressed within the context of LQR, this is not the case for *Mountain Car (Continuous)* and *Pendulum* which require a nonlinear controller. We therefore partition the state space in the case of these RL tasks and consider a corresponding piecewise-LQR controller where the learned variable vectors may differ or be shared across the partitions. Such details are provided below for *Mountain Car (Continuous)* and *Pendulum*.

B.1. *Cart Pole* under CBRL LQR

Environment. As depicted in Figure 2 and described in Section 3.1, *Cart Pole* consists of a pole connected to a horizontally moving cart with the goal of balancing the pole by applying a force on the cart to the left or right. The state of the system is given by $x = [p, \dot{p}, \theta, \dot{\theta}]$ in terms of the position of the cart p , the velocity of the cart \dot{p} , the angle of the pole θ , and the angular velocity of the pole $\dot{\theta}$.

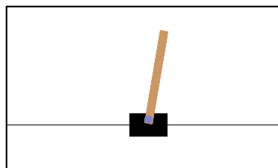


Figure 2: The *CartPole-v0* environment.

Controller. We address the *Cart Pole* problem within the context of our CBRL approach by exploiting the following general matrix form for the LQR dynamics

$$\dot{x} = \begin{bmatrix} \dot{p} \\ \ddot{p} \\ \dot{\theta} \\ \ddot{\theta} \end{bmatrix} = \underbrace{\begin{bmatrix} 0 & 1 & 0 & 0 \\ a_0 & a_1 & a_2 & a_3 \\ 0 & 0 & 0 & 1 \\ a_4 & a_5 & a_6 & a_7 \end{bmatrix}}_{A_v} x + \underbrace{\begin{bmatrix} 0 \\ b_0 \\ 0 \\ b_1 \end{bmatrix}}_{B_u} u, \quad (17)$$

which solely takes into account general physical relationships (e.g., the derivative of the angle of the pole is equivalent to its angular velocity) and laws (e.g., the force can only affect the acceleration), with the $d = 10$ unknown variables $a_0, \dots, a_7, b_0, b_1$ to be learned.

Numerical Results. Table 1 and Figure 3 present numerical results for the three state-of-the-art baselines (discrete actions) and our CBRL approach, each run over five independent random seeds. All variables in (17) are initialized uniformly within $(0, 1)$ and then learned using our control-policy-variable gradient ascent iteration (8). We consider four sets of initial variables (see Table 2) to validate the robustness of our CBRL approach. Figure 3(c) – 3(f) illustrates the learning behavior of CBRL variables given different initialization.

Table 1 and Figure 3(a) and 3(b) clearly demonstrate that our CBRL approach provides far superior performance, in terms of both mean and standard deviation, over all baselines w.r.t. both the number of episodes and running time, in addition to demonstrating a more stable training process. More specifically, our CBRL approach outperforms all baselines with a significant improvement in mean return over independent random environment runs from Gymnasium (Towers et al., 2023), together with a significant reduction in the standard deviation of the return over these independent runs, thus rendering a more robust solution approach where the performance of each run is much closer to the mean than under the corresponding baseline results. In fact, all independent random environment runs under our CBRL approach yield returns equal to the mean (i.e., standard deviation of 0) for episodes 150 and beyond. Moreover, the relative percentage difference¹ in improved mean return performance of our CBRL approach over the next-best RL method Linear (based on mean performance at 500 episodes) is 294% and 6.6% at 200 and 500 episodes, respectively; and the relative percentage difference in reduced standard deviation of return performance from the next-best RL method Linear to our CBRL approach is 200% and 200% at 200 and 500 episodes, respectively. In addition, the relative percentage difference in improved mean return performance of our CBRL approach over the DQN RL method is 927% and 29.5% at 200 and 500 episodes, respectively; and the relative percentage difference in reduced standard deviation of return performance from the DQN RL method to our CBRL approach is 200% and 200% at 200 and 500 episodes, respectively.

We note an important difference between Fig. 1(a) – 1(b) and Fig. 3(a) – 3(b), namely the shaded areas in Fig. 1(a) – 1(b) represent one form of variability across independent random seeds with the same variable initialization, whereas the shaded areas in Fig. 3(a) – 3(b) represent the combination of

1. For the relative comparison of improved mean return performance of our CBRL method over the next-best RL method, since all the performance values are positive, we use the standard relative percentage difference formula $\frac{M_{CBRL} - M_{RL}}{M_{RL}} \times 100$. Similarly, for the relative comparison of reduced standard deviation of return performance from the next-best RL method to our CBRL method, since all the performance values are positive, we typically use the standard relative percentage difference formula $\frac{S_{RL} - S_{CBRL}}{S_{CBRL}} \times 100$, with the sole exception of replacing the denominator with $(S_{RL} + S_{CBRL})/2$ based on the arithmetic mean when S_{CBRL} is zero. Refer to https://en.wikipedia.org/wiki/Relative_change

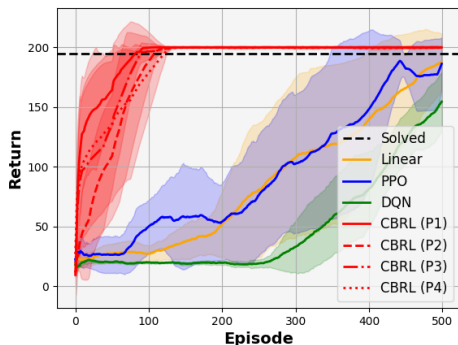
two forms of variability—one across independent random seeds with the same variable initialization and the other across different random variable initializations.

Table 1: Mean and Standard Deviation of Return of RL Methods for *CartPole-v0*

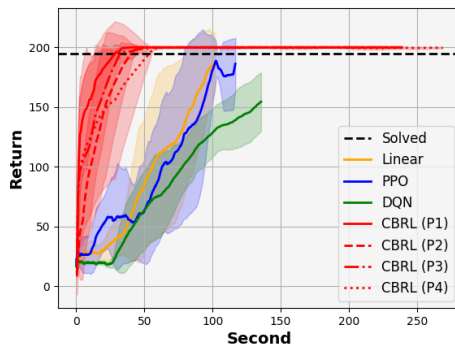
Episode Number	CBRL		Linear		PPO		DQN	
	Mean	Std. Dev.						
50	163.49	30.57	27.15	7.79	26.19	15.18	19.99	0.67
100	199.69	0.63	27.05	7.21	49.30	22.28	19.76	1.08
150	200.00	0.00	37.20	14.80	57.84	43.68	18.85	1.23
200	200.00	0.00	50.77	26.93	53.58	32.06	19.47	1.79
250	200.00	0.00	80.05	56.27	75.65	50.67	18.88	3.35
300	200.00	0.00	107.18	67.03	102.31	57.89	32.59	21.07
350	200.00	0.00	118.56	66.73	127.67	71.26	56.44	31.43
400	200.00	0.00	138.79	57.88	147.52	66.20	80.85	31.94
450	200.00	0.00	165.75	45.35	183.12	10.49	123.49	20.59
500	200.00	0.00	187.70	23.72	186.16	22.05	154.46	24.42

Table 2: Initial Variables of *CartPole-v0*

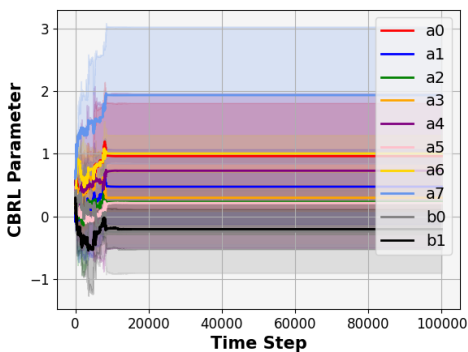
Name	a_0	a_1	a_2	a_3	a_4	a_5	a_6	a_7	b_0	b_1
Initial Variables 1 (P1)	0.436	0.026	0.55	0.435	0.42	0.33	0.205	0.619	0.3	0.267
Initial Variables 2 (P2)	0.076	0.78	0.438	0.723	0.978	0.538	0.501	0.072	0.268	0.5
Initial Variables 3 (P3)	0.154	0.74	0.263	0.534	0.015	0.919	0.901	0.033	0.957	0.137
Initial Variables 4 (P4)	0.295	0.531	0.192	0.068	0.787	0.656	0.638	0.576	0.039	0.358



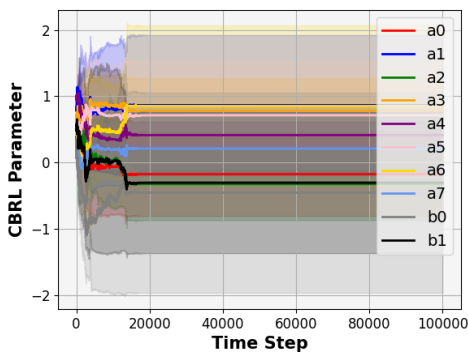
(a) Return vs. Episode



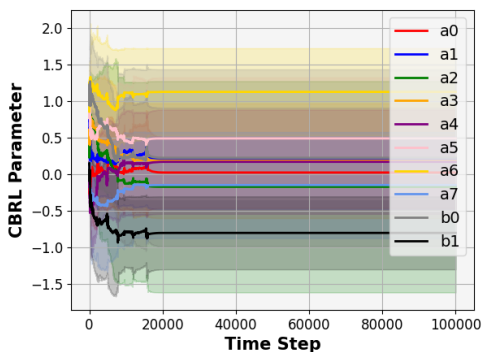
(b) Return vs. Time



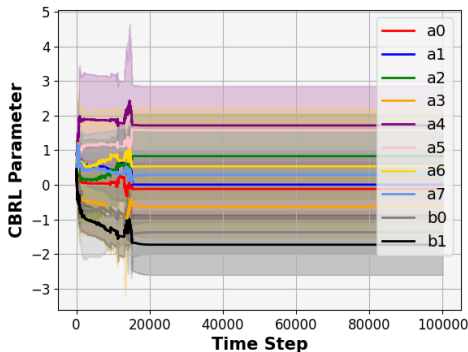
(c) P1



(d) P2



(e) P3



(f) P4

Figure 3: Learning curves of *CartPole-v0* over five independent runs. The solid line shows the mean and the shaded area depicts the standard deviation. (a) and (b): Return vs. number of episodes and running time, respectively, for our CBRL approach (over the five independent runs and the four initializations in Table 2) in comparison with the Linear policy, PPO, and DQN (over the five independent runs). (c) – (f): Learning behavior of CBRL variables, initialized by Table 2.

B.2. Lunar Lander (Continuous) under CBRL LQR

Environment. As depicted in Figure 4 and described in Section 3.2, *Lunar Lander (Continuous)* is a classical spacecraft trajectory optimization problem with the goal to land softly and fuel-efficiently on a landing pad by applying thrusters to the left, to the right, and upward. The state of the system is given by $x = [p_x, v_x, p_y, v_y, \theta, \dot{\theta}]$ in terms of the (x, y) positions p_x and p_y , two linear velocities v_x and v_y , angle θ , and angular velocity $\dot{\theta}$.

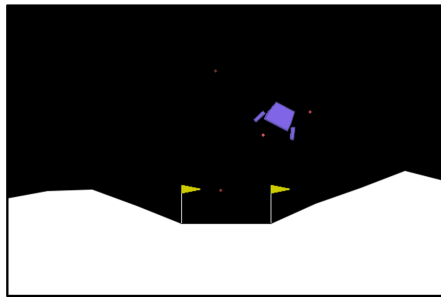


Figure 4: The *LunarLanderContinuous-v2* environment.

Controller. We address the *Lunar Lander (Continuous)* problem within the context of our CBRL approach by exploiting the following general matrix form for the LQR dynamics

$$\dot{x} = \begin{bmatrix} v_x \\ \ddot{p}_x \\ v_y \\ \ddot{p}_y \\ \dot{\theta} \\ \ddot{\theta} \end{bmatrix} = \underbrace{\begin{bmatrix} 0 & 1 & 0 & 0 & 0 & 0 \\ 0 & a_0 & 0 & a_1 & a_2 & a_3 \\ 0 & 0 & 0 & 1 & 0 & 0 \\ 0 & a_4 & 0 & a_5 & a_6 & a_7 \\ 0 & 0 & 0 & 0 & 0 & 1 \\ 0 & a_8 & 0 & a_9 & a_{10} & a_{11} \end{bmatrix}}_{A_v} x + \underbrace{\begin{bmatrix} 0 & 0 \\ 0 & b_0 \\ 0 & 0 \\ b_1 & 0 \\ 0 & 0 \\ 0 & b_2 \end{bmatrix}}_{B_v} u, \quad (18)$$

which solely takes into account general physical relationships (akin to *Cart Pole*) and mild physical information from the system state (e.g., the acceleration is independent of the position), with the $d = 15$ unknown variables $a_0, \dots, a_{11}, b_0, b_1, b_2$ to be learned.

Numerical Results. Table 3 and Figure 5 present numerical results for the three state-of-the-art baselines (continuous actions) and our CBRL approach, each run over five independent random seeds. All variables in (18) are initialized uniformly within $(0, 1)$ and then learned using our control-policy-variable gradient ascent iteration (8). We consider four sets of initial variables (see Table 4) to validate the robustness of our CBRL approach. Figure 5(c) – 5(f) illustrates the learning behavior of CBRL variables given different initialization.

Table 3 and Figure 5(a) and 5(b) clearly demonstrate that our CBRL approach provides far superior performance, in terms of both mean and standard deviation, over all baselines w.r.t. both the number of episodes and running time, in addition to demonstrating a more stable training process.

More specifically, our CBRL approach outperforms all baselines with a significant improvement in mean return over independent random environment runs from Gymnasium (Towers et al., 2023), together with a significant reduction in the standard deviation of the return over these independent runs, thus rendering a more robust solution approach where the performance of each run is much closer to the mean than under the corresponding baseline results. In fact, the relative percentage difference² in improved mean return performance of our CBRL approach over the next-best RL method DDPG (based on mean performance at 500 episodes) is 309% and 110% at 200 and 500 episodes, respectively; and the relative percentage difference in reduced standard deviation of return performance from the next-best RL method DDPG to our CBRL approach is 115% and 288% at 200 and 500 episodes, respectively. Moreover, the relative percentage difference in improved mean return performance of our CBRL approach over the PPO RL method is 361% and 390% at 200 and 500 episodes, respectively; and the relative percentage difference in reduced standard deviation of return performance from the PPO RL method to our CBRL approach is 639% and 559% at 200 and 500 episodes, respectively. We note that the baseline algorithms often crash and terminate sooner than the more successful landings of our CBRL approach, resulting in the significantly worse performance exhibited in Fig. 1(d) – 1(f), Table 3 and Figure 5.

We also note an important difference between Fig. 1(d) – 1(e) and Fig. 5(a) – 5(b), namely the shaded areas in Fig. 1(d) – 1(e) represent one form of variability across independent random seeds with the same variable initialization, whereas the shaded areas in Fig. 5(a) – 5(b) represent the combination of two forms of variability—one across independent random seeds with the same variable initialization and the other across different random variable initializations.

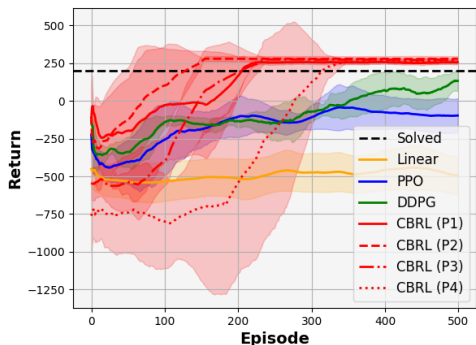
2. For the relative comparison of improved mean return performance of our CBRL method over the next-best RL method, since some of the performance values are negative and $|M_{RL}| < M_{CBRL}$, we use the standard relative percentage difference formula $\frac{M_{CBRL} - M_{RL}}{|M_{RL}|} \times 100$. Similarly, for the relative comparison of reduced standard deviation of return performance from the next-best RL method to our CBRL method, since all the performance values are positive, we use the standard relative percentage difference formula $\frac{S_{RL} - S_{CBRL}}{S_{CBRL}} \times 100$. Refer to https://en.wikipedia.org/wiki/Relative_change

Table 3: Mean and Standard Deviation of Return of RL Methods for *LunarLanderContinuous-v2*

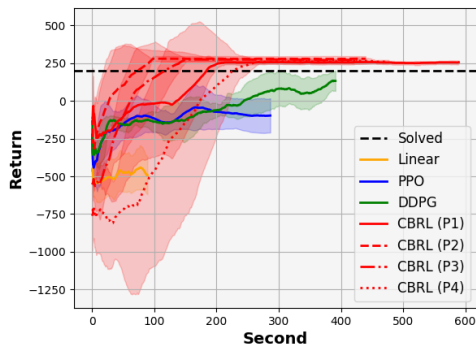
Episode Number	CBRL		Linear		PPO		DDPG	
	Mean	Std. Dev.						
50	-128.81	276.58	-531.05	115.63	-403.56	143.06	-337.22	98.64
100	101.33	262.09	-533.6	130.04	-260.08	238.84	-145.05	42.29
150	258.84	31.52	-510.13	123.56	-188.50	121.78	-154.48	43.2
200	279.24	18.12	-513.44	129.48	-106.87	133.97	-133.51	38.96
250	280.36	17.19	-475.43	125.81	-127.29	81.82	-143.46	112.20
300	279.19	18.42	-473.77	127.78	-109.72	79.65	-73.1	70.24
350	280.08	17.14	-479.01	124.67	-45.12	140.02	-9.04	98.49
400	279.51	17.67	-458.10	131.61	-75.52	111.54	70.04	120.93
450	278.96	19.22	-445.52	143.65	-91.77	105.02	51.15	99.21
500	280.09	17.16	-492.67	126.01	-96.50	113.10	133.20	66.54

Table 4: Initial Variables of *LunarLanderContinuous-v2*

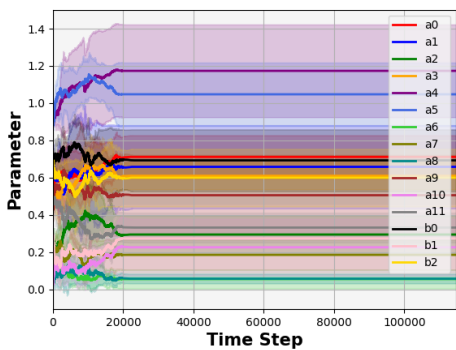
Name	a_0	a_1	a_2	a_3	a_4	a_5	a_6	a_7
Initial Variables 1 (P1)	0.551	0.708	0.291	0.511	0.893	0.896	0.126	0.207
Initial Variables 2 (P2)	0.873	0.969	0.869	0.531	0.233	0.011	0.43	0.402
Initial Variables 3 (P3)	0.778	0.238	0.824	0.966	0.973	0.453	0.609	0.776
Initial Variables 4 (P4)	0.65	0.505	0.879	0.182	0.852	0.75	0.666	0.988
Name	a_8	a_9	a_{10}	a_{11}	b_0	b_1	b_2	
Initial Variables 1 (P1)	0.051	0.441	0.03	0.457	0.649	0.278	0.676	
Initial Variables 2 (P2)	0.523	0.478	0.555	0.543	0.761	0.712	0.62	
Initial Variables 3 (P3)	0.642	0.722	0.035	0.298	0.059	0.857	0.373	
Initial Variables 4 (P4)	0.257	0.028	0.636	0.847	0.736	0.021	0.112	



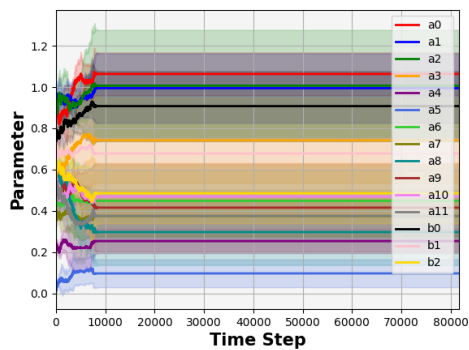
(a) Return vs. Episode



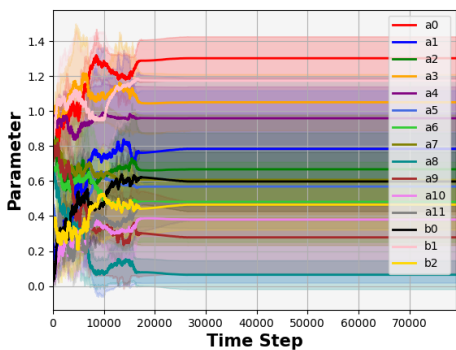
(b) Return vs. Time



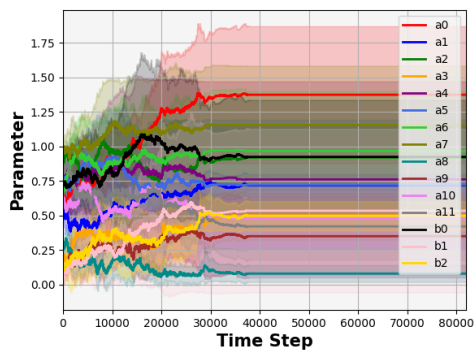
(c) P1



(d) P2



(e) P3



(f) P4

Figure 5: Learning curves of *LunarLanderContinuous-v2* over five independent runs. The solid line shows the mean and the shaded area depicts the standard deviation. (a) and (b): Return vs. number of episodes and running time, respectively, for our CBRL approach (over the five independent runs and the four initializations in Table 4) in comparison with the Linear policy, PPO, and DDPG (over the five independent runs). (c) – (f): Learning behavior of CBRL variables, initialized by Table 4.

B.3. Mountain Car (Continuous) under CBRL Piecewise-LQR

Environment. As depicted in Figure 6 and described in Section 3.3, *Mountain Car (Continuous)* consists of a car placed in a valley with the goal of accelerating the car to reach the target at the top of the hill on the right by applying a force on the car to the left or right. The state of the system is given by $x = [p, v]$ in terms of the position of the car p and the velocity of the car v .

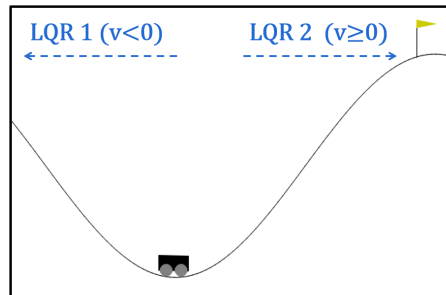


Figure 6: The *MountainCarContinuous-v0* environment and partitions for piecewise-LQR.

Controller. Recall that the LQR controller is not sufficient to solve the *Mountain Car (Continuous)* problem, even if all the variables of the system are known (e.g., mass of the car and gravity), because a nonlinear controller is required. Consequently, we consider a piecewise-LQR controller that partitions the state space into two regions: LQR 1 and LQR 2 (see Figure 6). The target state $x^* = [p^*, v^*]$ for LQR 1 and LQR 2 are respectively selected as $x^* = [-1.2, 0]$ and $x^* = [0.6, 0]$, where -1.2 and 0.6 correspondingly represent the position of the left hill and the right hill. We address the problem within the context of our CBRL approach by exploiting the following general matrix form for the piecewise-LQR dynamics

$$\dot{e} = \begin{bmatrix} v - v^* \\ \dot{v} - \dot{v}^* \end{bmatrix} = \begin{bmatrix} 0 & 1 \\ a_0 \sin(3p^*) & a_1 \end{bmatrix} e + \begin{bmatrix} 0 \\ b_0 \end{bmatrix} (u - c_0 \cos(3p^*)), \quad (19)$$

which solely takes into account general physical relationships and laws, with the $d = 4$ unknown variables a_0, a_1, b_0, c_0 to be learned where $e = x - x^*$ and we select $v^* = 0, \dot{v}^* = 0$, and $p^* = -1.2$ or 0.6 .

Numerical Results. Table 5 and Figure 7 present numerical results for the three state-of-the-art baselines (continuous actions) and our CBRL approach, each run over five independent random seeds. All variables in (19) are initialized uniformly within $(0, 1)$ and then learned using our control-policy-variable gradient ascent iteration (8). We consider four sets of initial variables (see Table 6) to validate the robustness of our CBRL approach. Figure 7(c) – 7(f) illustrates the learning behavior of CBRL variables given different initialization.

Table 5 and Figure 7(a) and 7(b) clearly demonstrate that our CBRL approach provides superior performance, in terms of both mean and standard deviation, over all baselines w.r.t. both the number of episodes and running time, in addition to demonstrating a more stable training process. More specifically, our CBRL approach outperforms all baselines with a significant improvement in mean return over independent random environment runs from Gymnasium (Towers et al., 2023), together with a significant reduction in the standard deviation of the return over these independent runs, thus

rendering a more robust solution approach where the performance of each run is much closer to the mean than under the corresponding baseline results. In fact, the relative percentage difference³ in improved mean return performance of our CBRL approach over the next-best RL method DDPG (based on mean performance at 500 episodes) is 0.9% and 1% at 200 and 500 episodes, respectively; and the relative percentage difference in reduced standard deviation of return performance from the next-best RL method DDPG to our CBRL approach is 324% and 257% at 200 and 500 episodes, respectively. Moreover, the relative percentage difference in improved mean return performance of our CBRL approach over the PPO RL method is 41% and 23% at 200 and 500 episodes, respectively; and the relative percentage difference in reduced standard deviation of return performance from the PPO RL method to our CBRL approach is 5743% and 729% at 200 and 500 episodes, respectively.

We note an important difference between Fig. 1(g) – 1(h) and Fig. 7(a) – 7(b), namely the shaded areas in Fig. 1(g) – 1(h) represent one form of variability across independent random seeds with the same variable initialization, whereas the shaded areas in Fig. 7(a) – 7(b) represent the combination of two forms of variability—one across independent random seeds with the same variable initialization and the other across different random variable initializations.

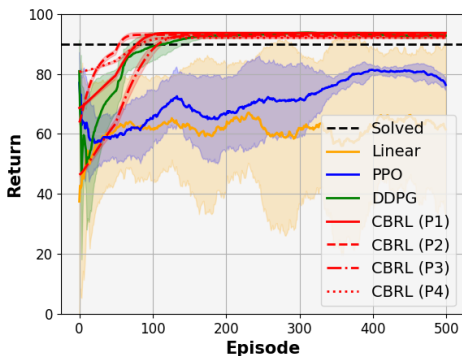
Table 5: Mean and Standard Deviation of Return of RL Methods for *MountainCarContinuous-v0*

Episode Number	CBRL		Linear		PPO		DDPG	
	Mean	Std. Dev.	Mean	Std. Dev.	Mean	Std. Dev.	Mean	Std. Dev.
50	79.34	1.02	61.09	16.84	59.62	7.32	74.20	7.20
100	93.03	0.37	61.64	17.19	65.01	9.69	89.10	4.78
150	93.63	0.21	63.12	19.53	69.58	10.57	91.98	1.47
200	93.63	0.21	61.94	21.83	66.36	12.27	92.82	0.89
250	93.63	0.21	62.30	25.59	71.35	13.15	93.18	0.41
300	93.63	0.21	62.00	25.12	71.25	12.27	93.62	0.35
350	93.63	0.21	57.13	34.55	76.23	3.03	93.39	0.51
400	93.63	0.21	62.42	25.91	81.32	1.63	93.15	0.81
450	93.63	0.21	66.19	20.54	81.10	2.02	92.67	0.85
500	93.63	0.21	61.52	28.84	76.31	1.74	92.72	0.75

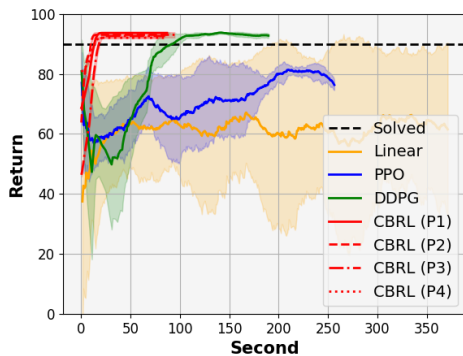
3. For the relative comparison of improved mean return performance of our CBRL method over the next-best RL method, since all the performance values are positive, we use the standard relative percentage difference formula $\frac{M_{CBRL} - M_{RL}}{M_{RL}} \times 100$. Similarly, for the relative comparison of reduced standard deviation of return performance from the next-best RL method to our CBRL method, since all the performance values are positive, we use the standard relative percentage difference formula $\frac{S_{RL} - S_{CBRL}}{S_{CBRL}} \times 100$. Refer to https://en.wikipedia.org/wiki/Relative_change

Table 6: Initial Variables of *MountainCarContinuous-v0*

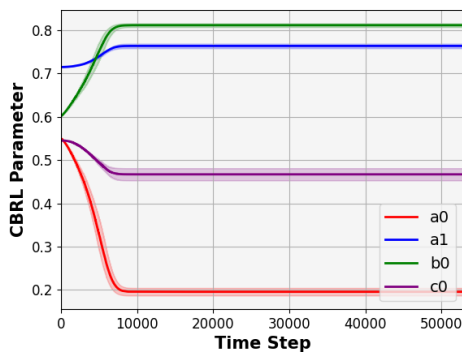
Name	a_0	a_1	b_0	c_0
Initial Variables 1 (P1)	0.549	0.715	0.603	0.545
Initial Variables 2 (P2)	0.222	0.871	0.207	0.919
Initial Variables 3 (P3)	0.771	0.021	0.634	0.749
Initial Variables 4 (P4)	0.588	0.898	0.892	0.816



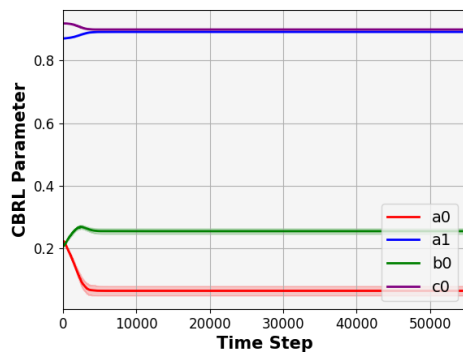
(a) Return vs. Episode



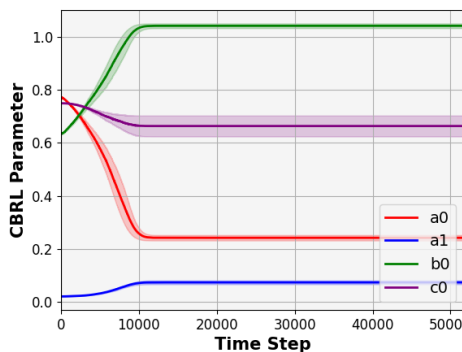
(b) Return vs. Time



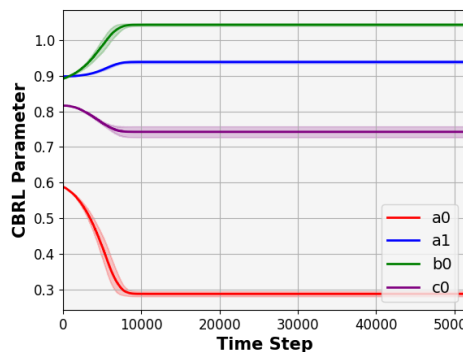
(c) P1



(d) P2



(e) P3



(f) P4

Figure 7: Learning curves of *MountainCarContinuous-v0* over five independent runs. The solid line shows the mean and the shaded area depicts the standard deviation. (a) and (b): Return vs. number of episodes and running time, respectively, for our CBRL approach (over the five independent runs and the four initializations in Table 6) in comparison with the Linear policy, PPO, and DDPG (over the five independent runs). (c) – (f): Learning behavior of CBRL variables, initialized by Table 6.

B.4. *Pendulum* under CBRL Piecewise-LQR

Environment. As depicted in Figure 8 and described in Section 3.4, *Pendulum* consists of a link attached at one end to a fixed point and the other end being free, with the goal of swinging up to an upright position by applying a torque on the free end. The state of the system is given by $x = [\theta, \dot{\theta}]$ in terms of the angle of the link θ and the angular velocity of the link $\dot{\theta}$.

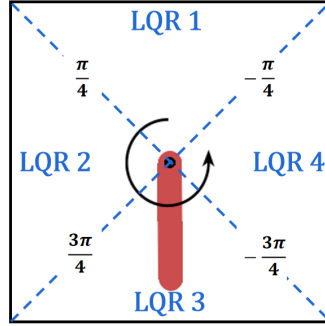


Figure 8: The *Pendulum-v1* environment and partitions for piecewise-LQR.

Controller. Recall that the LQR controller is not sufficient to solve the *Pendulum* problem, even if all the variables of the system are known (e.g., mass of the link m , length of the link l , moment of inertia of the link J , and gravity g), because a nonlinear controller is required. Consequently, we consider a piecewise-LQR controller that partitions the state space into four regions: LQR 1, LQR 2, LQR 3, LQR 4 (see Figure 8). In terms of the target state $x^* = [\theta^*, \dot{\theta}^*]$, θ^* is selected based on the boundary angle in each partition (counter-clockwise boundary angle if $\dot{\theta} > 0$, and clockwise boundary angle otherwise), while $\dot{\theta}^*$ is selected based on the energy conservation law. More specifically, θ^* in LQR 1 is selected to be $\theta^* = \pi/4$ if $\dot{\theta} > 0$, and to be $\theta^* = -\pi/4$ otherwise. Given the assumption that the link reaches a zero velocity at the upright position, $\dot{\theta}^*$ is selected at any position to be $\dot{\theta}^* = \sqrt{mgl(1 - \cos(\theta))/J}$. We address the problem within the context of our CBRL approach by exploiting the following general matrix form for the piecewise-LQR dynamics

$$\dot{e} = \begin{bmatrix} \dot{\theta} - \dot{\theta}^* \\ \ddot{\theta} - \ddot{\theta}^* \end{bmatrix} = \begin{bmatrix} 0 & 1 \\ a_0 \cos(\theta^*) & a_1 \end{bmatrix} e + \begin{bmatrix} 0 \\ b_0 \end{bmatrix} (u + c_0 \sin(\theta^*)), \quad \dot{\theta}^* = \sqrt{d_0(1 - \cos(\theta))}, \quad (20)$$

which solely takes into account general physical relationships and laws, with the $d = 5$ unknown variables a_0, a_1, b_0, c_0, d_0 to be learned where $e = x - x^*$ and we select $\ddot{\theta}^* = 0$.

Numerical Results. Table 7 and Figure 9 present numerical results for the three state-of-the-art baselines (continuous actions) and our CBRL approach, each run over five independent random seeds. All variables in (20) are initialized uniformly within $(0, 1)$ and then learned using our control-policy-variable gradient ascent iteration (8). We consider four sets of initial variables (see Table 8) to validate the robustness of our CBRL approach. Figure 9(c) – 9(f) illustrates the learning behavior of CBRL variables given different initialization.

Table 7 and Figure 9(a) and 9(b) clearly demonstrate that our CBRL approach provides far superior performance, in terms of both mean and standard deviation, over all baselines w.r.t. both

the number of episodes and running time upon convergence of our CBRL algorithm after a relatively small number of episodes, in addition to demonstrating a more stable training process. More specifically, even with only four partitions for the difficult nonlinear *Pendulum* RL task, our CBRL approach outperforms all baselines after 150 episodes with a significant improvement in mean return over independent random environment runs from Gymnasium (Towers et al., 2023), together with a significant reduction in the standard deviation of the return over these independent runs, thus rendering a more robust solution approach where the performance of each run is much closer to the mean than under the corresponding baseline results. In fact, the relative percentage difference⁴ in improved mean return performance of our CBRL approach over the next-best RL method DDPG (based on mean performance at 500 episodes) is 40% and 53% at 200 and 500 episodes, respectively; and the relative percentage difference in reduced standard deviation of return performance from the next-best RL method DDPG to our CBRL approach is 210% and 263% at 200 and 500 episodes, respectively. Moreover, the relative percentage difference in improved mean return performance of our CBRL approach over the PPO RL method is 197% and 168% at 200 and 500 episodes, respectively; and the relative percentage difference in reduced standard deviation of return performance from the PPO RL method to our CBRL approach is 275% and 793% at 200 and 500 episodes, respectively.

We note an important difference between Fig. 1(j) – 1(k) and Fig. 9(a) – 9(b), namely the shaded areas in Fig. 1(j) – 1(k) represent one form of variability across independent random seeds with the same variable initialization, whereas the shaded areas in Fig. 9(a) – 9(b) represent the combination of two forms of variability—one across independent random seeds with the same variable initialization and the other across different random variable initializations.

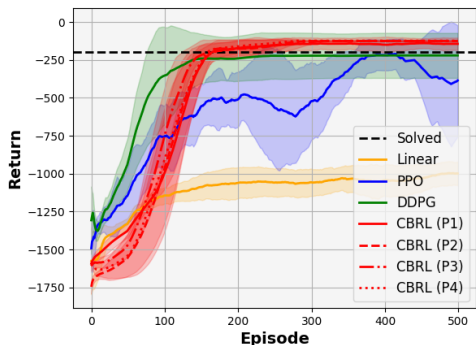
4. For the relative comparison of improved mean return performance of our CBRL method over the next-best RL method, since all the performance values are negative, we use the reversed standard relative percentage difference formula $\frac{|M_{RL} - M_{CBRL}|}{|M_{CBRL}|} \times 100$. Similarly, for the relative comparison of reduced standard deviation of return performance from the next-best RL method to our CBRL method, since all the performance values are positive, we use the standard relative percentage difference formula $\frac{S_{RL} - S_{CBRL}}{S_{CBRL}} \times 100$. Refer to https://en.wikipedia.org/wiki/Relative_change

Table 7: Mean and Standard Deviation of Return of RL Methods for *Pendulum-v1*

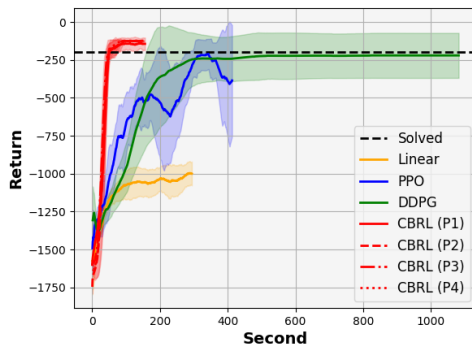
Episode Number	CBRL		Linear		PPO		DDPG	
	Mean	Std. Dev.	Mean	Std. Dev.	Mean	Std. Dev.	Mean	Std. Dev.
50	-1378.78	43.89	-1331.73	36.25	-1147.35	181.20	-942.18	170.83
100	-1004.75	101.66	-1145.30	53.57	-757.11	205.66	-355.09	324.16
150	-284.26	130.17	-1088.67	83.73	-559.65	151.39	-241.16	162.85
200	-172.48	48.32	-1062.06	102.63	-511.85	181.28	-240.94	149.57
250	-152.80	37.43	-1058.88	92.55	-561.78	384.15	-222.18	151.71
300	-145.56	44.16	-1057.02	90.29	-524.10	259.46	-221.78	150.40
350	-141.80	36.63	-1036.65	88.37	-325.66	133.77	-222.83	146.68
400	-149.34	51.70	-1044.34	100.90	-218.37	100.83	-220.28	148.80
450	-139.65	32.36	-1032.82	87.11	-296.94	184.32	-220.50	148.68
500	-143.95	40.91	-999.41	78.75	-385.50	365.39	-220.38	148.54

Table 8: Initial Variables of *Pendulum-v1*

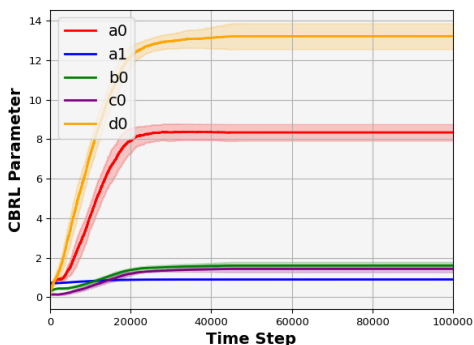
Name	a_0	a_1	b_0	c_0	d_0
Initial Variables 1 (P1)	0.417	0.72	0.302	0.147	0.092
Initial Variables 2 (P2)	0.893	0.332	0.821	0.042	0.108
Initial Variables 3 (P3)	0.18	0.019	0.463	0.725	0.42
Initial Variables 4 (P4)	0.223	0.523	0.551	0.046	0.361



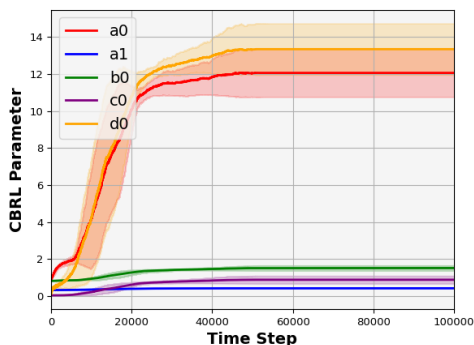
(a) Return vs. Episode



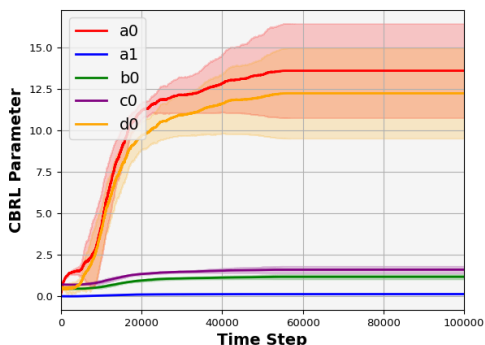
(b) Return vs. Time



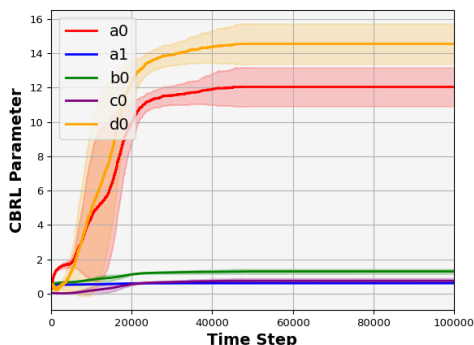
(c) P1



(d) P2



(e) P3



(f) P4

Figure 9: Learning curves of *Pendulum-v1* over five independent runs. The solid line shows the mean and the shaded area depicts the standard deviation. (a) and (b): Return vs. number of episodes and running time, respectively, for our CBRL approach (over the five independent runs and the four initializations in Table 8) in comparison with the Linear policy, PPO, and DDPG (over the five independent runs). (c) – (f): Learning behavior of CBRL variables, initialized by Table 8.

B.5. Implementation

Baselines. As previously noted, the evaluation of our CBRL approach includes comparisons against the three baselines of DQN for discrete actions, DDPG for continuous actions and PPO, which are selected as the state-of-the-art RL algorithms for solving the RL tasks under consideration. The additional baseline of replacing the nonlinear policy of PPO with a linear policy was again included because the optimal policy for some problems, e.g., *Cart Pole*, is known to be linear. This Linear algorithm solely replaces the policy network of PPO with a linear policy while maintaining all other components unchanged. More specifically, we decrease the number of hidden layers in the policy network by 1, reduce the hidden layer size of the policy network to 16, and remove all (nonlinear) activation functions in the policy network.

Hyperparameters. We summarize in Table 9 the hyperparameters that have been used in our numerical experiments. To ensure a fair comparison, we maintain consistent hyperparameters (e.g., hidden layer size of the value network and the activation function) across all algorithms wherever applicable.

Table 9: Summary of Experimental Hyperparameters

Algorithm	Linear	PPO	DDPG	DQN	CBRL
Action Generator	NN	NN	NN	NN	CBRL-LQR
# of Hidden Layers (Policy)	1	2	2	2	N/A
# of Hidden Layers (Value)	2	2	2	2	2
Hidden Layer Size (Policy)	16	128	128	128	N/A
Hidden Layer Size (Value)	128	128	128	128	128
Activation (Policy)	N/A	ReLU & Tanh	ReLU & Tanh	ReLU & Tanh	N/A
Activation (Value)	ReLU	ReLU	ReLU	ReLU	ReLU
Discount Factor	0.99	0.99	0.99	0.99	0.99
Clip Ratio	0.2	0.2	N/A	N/A	N/A
Soft Update Ratio	N/A	N/A	0.005	N/A	N/A